# Cardioprotective effects of Hph1-PLCδ1 protein transduction in ischemia/reperfusion injury and its mechanisms

Soyeon Lim

Department of Medical Science

The Graduate School, Yonsei University

# Cardioprotective effects of Hph1-PLCδ1 protein transduction in ischemia/reperfusion injury and its mechanisms

Directed by Professor Yangsoo Jang

Doctoral Dissertation

submitted to the Department of Medical Science,

the Graduate School of Yonsei University

in partial fulfillment of the requirements

for the degree of Doctor of Philosophy

Soyeon Lim

December 2007

This certifies that the Doctoral Dissertation

of Soyeon Lim is approved.

_____

Thesis Supervisor: Dr.Yangsoo Jang

_____

Thesis committee Member: Dr. Ki-Chul Hwang

_____

Thesis committee Member: Dr. Donghoon Choi

_____

Thesis committee Member: Dr. Duck Sun Ahn

_____

Thesis committee Member: Dr. Jong Eun Lee

# The Graduate School

# Yonsei University

December 2007

# Acknowledgements

# TABLE OF CONTENTS

iii

# LIST OF FIGURES

iv

# LIST OF TABLES

Abstract

# Cardioprotective effects of Hph1-PLCδ1 protein transduction in ischemia/reperfusion injury and its mechanisms

Soyeon Lim

*Department of Medical Science*

*The Graduate School, Yonsei University*

(Directed by Professor Yangsoo Jang)

Myocardial oxidative stress and $Ca^{2+}$ overload induced by ischemia/ reperfusion (I/R) may be involved in the development and progression of myocardial dysfunction in heart failure. Phospholipase C (PLC) plays an important role in the regulation of the phosphoinositol pathway and $Ca^{2+}$ homeostasis in many cells, especially those of the heart. PLCδ1 is degraded in

ischemic heart tissue and hypoxic neonatal cardiomyocytes, leading to intracellular $Ca^{2+}$ overload. This study was designed to determine whether the PLCδ1 protein has cardioprotective effects against myocardial ischemia/ reperfusion injury by restoration of PLCδ1 and, if so, to determine the mechanism by which this occurs. We used a novel cell-permeable protein transduction domain (PTD), Hph1, to delivery PLCδ1 as a treatment for myocardial ischemia/reperfusion injury. In hypoxic/reoxygenated cardiomyocytes, transduction of Hph1-PLCδ1 inhibited significant intracellular $Ca^{2+}$ overload, mitochondrial permeability transition pore (mPTP) opening, and change of the mitochondrial membrane potential. Hph1-PLCδ1, also, affected expression of the $Na^{+}$-$Ca^{2+}$ exchanger and the ryanodine receptor in $H_2O_2$-stimulated cardiomyocytes. Finally, Hph1-PLCδ1 inhibited apoptosis through the regulation of cytochrome C, caspase 3, pro-apoptotic factor Bax, and anti-apoptotic factor Bcl-2. Echocardiography and histological examination were performed on Spraque-Dawley (SD) rat hearts two weeks after reperfusion. In contrast to the I/R control group, the intravenous injection group of Hph1-PLCδ1 experienced a significant reduction in infarct size and apoptosis and an improvement in systolic and diastolic cardiac

function. These results suggest that transduction of Hph1-PLCδ1 reduces myocardial dysfunction by preventing the mitochondrial apoptotic pathway in cells suffering ischemia/reperfusion injury.

---

# Cardioprotective effects of Hph1-PLCδ1 protein transduction in ischemia/reperfusion injury and its mechanisms

Soyeon Lim

*Department of Medical Science*

*The Graduate School, Yonsei University*

(Directed by Professor Yangsoo Jang)

## I. INTRODUCTION

A constant supply of oxygen from the coronary arteries and cellular calcium homeostasis are important for the regulation of heart function. It is well known that a reduction in oxygen supply by coronary artery obstruction causes myocardial ischemia, leading to cardiac dysfunction [1, 2]. Although treatments for the restoration of blood flow, such as coronary surgery,

angioplasty, and thrombolytic therapy, are essential to lessen the ischemic insult, these procedures can generate a reperfusion injury, which may result in myocardial death [3, 4, 5]. Li et al. reported that reperfusion accelerates cellular apoptosis induced by hypoxia [6]. Therefore, control of reperfusion injury is a very important factor in myocardial survival.

Although coronary artery bypass grafting (CABG) and percutaneous intervention (PCI) are representative treatments of ischemic heart disease of the 1960's and 1970's, these procedures have several side effects, including coronary flow limitation and restenosis, which are primarily due to ischemia/reperfusion injury in the early phase [7, 8, 9, 10]. Thayssen reported that the rate of restenosis was 15-50% within eight months [11]. To solve these severe problems, drug-eluting stents (DESs) were introduced, and the incidence of restenosis decreased. However, there are still two problems: subacute stent thrombosis and a high restenosis rate. Also, it was reported that the long-term therapeutic effects of bare-metal stents and drug-eluting stents were not different in regard to the rates of death and myocardial infarction [12]. In addition, antioxidants, including natural products, and recombinant genes have been used for apoptosis inhibition in ischemic/reperfused

cardiomyocytes [13, 14]. Recently, Trimetazine, a metabolic agent, was used to inhibit apoptosis in ischemia/reperfusion injury [15].

Ischemia/reperfusion injury leads to the formation of reactive oxygen species (ROS), neutrophil activation, a decrease in the ATP concentration, and $Ca^{2+}$ overload. ROS, consisting of the superoxide anion, hydrogen peroxide, and the hydroxyl radical, have been implicated as major initiators of myocardial injury and apoptosis during reperfusion [16, 17, 18, 19, 20]. This concept was demonstrated when treatment with antioxidants significantly reduced myocardial apoptosis after reperfusion [21]. Both intrinsic and extrinsic signaling mechanisms related to ROS-triggered apoptosis are generally understood. The intrinsic pathway is initiated by intracellular $Ca^{2+}$ overload, which is induced by ROS production [22, 23, 24, 25]. Under physiological conditions, calcium is a key regulator of mitochondrial function and regulates ATP synthesis at several organelle levels [26]. However, in the presence of a pathologic stimulus, a rise in the $Ca^{2+}$ concentration in the cytoplasm leads to $Ca^{2+}$ transport into the mitochondria. A high $Ca^{2+}$ concentration may induce opening of mitochondrial permeability transition pores (mPTPs), which leads to the activation of numerous cytosolic proteins, phospholipases, protein

kinases, proteases, and endonucleases [27]. Calcium-activated proteases destroy the proteins that regulate intracellular calcium levels, thereby, decreasing calcium responsiveness. This eventually induces hypertrophy, heart failure, and apoptosis. Furthermore, apoptosis is promoted by mitochondrial ROS generation during the apoptotic process. The extrinsic pathway is associated with the generation of exogenous and endogenous ROS from cellular sources (neutrophils, macrophages, and endothelial cells) and mitochondria following $Ca^{2+}$ overload. This activates MAPKs (p38 and JNK MAPKs) [28, 29, 30] and elicits dissociation of NF-κB from its inhibitor IκB in the cytosol, which goes on to form active NF-κB in the nucleus [31]. NF-κB promotes synthesis of TNF-α. TNF-α is released from the cell, at which point it combines with membrane surface receptors (TNFR1 and Fas) to initiate an extrinsic and receptor-dependent death cascade.

Since the molecular mechanism of mPTP opening was found in the 1980s by Martin Crompton [32], many researchers have reported that mPTP opening is closely related to cell death in reperfusion. Since then, inhibition of mPTP opening has been focused on as a possible treatment for heart disease [33, 34, 35]. In an experiment with transgenic mice lacking CyP-D, one of the elements

necessary for the opening of the mPTP, there was a marked reduction in the rate of apoptosis after exposure to ischemia/reperfusion [36]. The mPTP is a voltage-dependent channel formed at the inner mitochondrial membrane. It has a diameter of 3 nm in the fully open state and allows passive diffusion of solutes less than 1.5 kDa in size [37]. The mPTP is a channel complex that consists of a voltage-dependent anion channel (VDAC) in the outer membrane, an adenine nucleotide translocator (ANT) in the inner membrane, cyclophilin D (Cyp D), and other molecules [32]. The mPTP is closed under ischemic conditions but opens with reperfusion. The reversibility of mPTP opening in reperfusion may determine the type of ensuing cell death, either apoptosis or necrosis [38, 39]. Cyclosporine A (CsA) and sanglifehrin (SfA) are representative immunosuppressant drugs and are inhibitors of mPTP opening. They bind to CyP-D and block mPTP opening by inhibiting the conformational change catalyzed by CyP-D [40]. Other than the aforementioned drugs, there are many other factors that affect the opening of mPTPs. Butylhydroxytoluene, an antioxidant, is a major inhibitor of mPTP opening. Conditions that occur in a state of hypoxia, such as a decreased ATP/ADP ratio, adenosine nucleotide depletion, and decreased intracellular pH, also, inhibit mPTP opening [41].

In a previous study, we reported that phospholipase C (PLC) $\delta$1 (not $\beta$1 or $\gamma$1) was selectively degraded in rat heart tissue *in vivo* and *in vitro* under hypoxic conditions [42]. Degradation of PLC$\delta$1 was blocked by treatment with calpastatin, a calpain inhibitor, and zVAD-fmk, a caspase pseudosubstrate inhibitor, in hypoxic neonatal cardiomyocytes. Over-expression of PLC$\delta$1 and treatment with calpastatin rescued cardiomyocytes from intracellular $Ca^{2+}$ overload in hypoxia. Therefore, maintenance of PLC$\delta$1 levels is a potential method of protein therapy in ischemic/reperfused heart tissue.

PLC$\delta$1 is the most abundant and widely expressed isoform of PLC$\delta$ in mammals. PLC$\delta$ isoforms are the most sensitive to $Ca^{2+}$ because they have several negatively charged residues within their catalytic domains [43]. Phospholipase C (PLC) plays an important role in the phosphoinositol pathway and $Ca^{2+}$ homeostasis regulation in many cells, including cardiomyocytes [44, 45, 46]. PLC$\delta$1 is stimulated by PLC$\beta$ or PLC$\gamma$ and costimulated by TGII/$G_h$ in response to a rise in intracellular $Ca^{2+}$ [47]. PLC, once activated, hydrolyzes phosphatidylinositol 4,5-biphosphate (PIP$_2$), forming two second messengers, inositol 1,4,5-triphosphate [I(1,4,5)P$_3$] and 1,2-diacyglycerol (DAG). I(1,4,5)P$_3$ directly stimulates an increase in

cytosolic $Ca^{2+}$ through interactions with $I(1,4,5)P_3$ receptors on the endoplasmic reticulum, whereas DAG activates protein kinase C, another critical component in cellular $Ca^{2+}$ maintenance [48]. Additionally, PLCδ1 is important not only for normal regulation of cellular proliferation and differentiation, but for determination of skin stem cell fate *in vivo* [50]. However, despite some understanding of the molecule in general, its biological and physiological functions in ischemia/reperfusion are not well understood.

Protein transduction domains (PTDs) were used to rapidly introduce PLCδ1 to cells undergoing reperfusion, as a therapeutic application. PTDs are small protein domains that are essential for viral replication. Fusion proteins composed of PTDs can be powerful tools for the delivery of therapeutic proteins to eukaryotic cells [51, 52]. PTD fusion proteins can transduce proteins ranging in size from 15 to 120 kDa into a variety of human and murine cells. Their use affords many important advantages, such as high transduction efficiency, rapid cellular uptake, and low toxicity, relative to previously used gene delivery methods in primary non-dividing cells [53]. Therefore, a novel cell-permeable PTD, YARVRRRGRRR, from a human transcriptional factor, Hph1, was used to introduce the PLCδ1 protein into cardiomyocytes.

Therefore, the hypothesis of this study was that cell death induced by H/R or I/R in cardiomyocytes is mediated by mPTP opening, and this is closely related to selective degradation of PLCδ1. Administration of the Hph1-PLCδ1 fusion protein will lead to increased rates of cell survival through regulation of mPTP opening in hypoxia/reoxygenation (H/R) and will inhibit apoptosis of cardiomyocytes in ischemia/reperfusion (I/R). To test this hypothesis, Hph1-PLCδ1 fusion proteins were used to directly protect again I/R injury *in vivo* and *in vitro*. A new method, which was a modified version of one previously created by Petronilli, was used to detect mPTP opening. This modified method was useful in quantifying mPTP opening in multiple conditions, without mitochondrial isolation or image analysis [54, 55].

## II. MATERIALS AND METHODS

### 1. Isolation and culture of rat cardiomyocytes

Neonatal rat cardiomyocytes were prepared by an enzymatic method [48, 56]. Briefly, hearts of one- to two-day-old Sprague-Dawley (SD) rat pups were dissected, minced, enzymatically dispersed with 10 ml of collagenase II (0.5 mg/ml, 262 U/mg, Gibco BRL, Paisley, UK), and centrifuged differentially to yield $5\times10^5$ cells/mL. After incubation for 4-6 h, the cells were rinsed twice with α-MEM containing 10 % fetal bovine serum (FBS) (Gibco BRL, Paisley, UK), and 0.1 μM BrdU (Sigma Chemical Co., St. Louis, MO, U.S.A) was added to inhibit fibrous growth. Cells were then cultured in a $CO_2$ incubator at 37 °C for 1 day for the treatment of hypoxia/reoxygenation.

### 2. Purification of Hph1-PLCδ1 proteins

The expression plasmid pHph1-PLCδ1 was transformed by a heat shock transformation method to BL21-DE3 (ATCC N. 53863). The transformed bacteria were grown to $OD_{600}$ 0.7 in LB medium. Protein expression was induced at 37 °C with 1 mM IPTG (Gibco BRL, Paisley, UK) for 4 h. The cells were harvested by centrifugation at 6000 rpm for 20 min, and the pellet

was resuspended in the binding buffer (50 mM $NaH_2PO_4$, 300 mM NaCl, 10 mM Imidazole, pH 8.0). The bacteria were then sonicated for 6s with an on/off total time of 8 min (Heat systems, ultrasonic processor XL). After removal of the cell debris by centrifugation, 0.5 mL of 50 % $Ni^{2+}$-NTA agarose beads (Qiagen, Hilden, Germany) was added to the clarified cell extract. Binding on agarose beads was performed at 4 °C. The extract was loaded onto a poly-Prep chromatography column (0.8×4, BioRad, CA, USA). The column was washed with wash buffer (20 mM Tris-HCl, 500 mM NaCl, 20 mM Imidazole, pH 7.9) and eluted by 1 mL each of elution buffer 1 (50 mM $NaH_2PO_4$, 300 mM NaCl, 250 mM Imidazole, pH 8.0)) and elution buffer 2 (50 mM $NaH_2PO_4$, 300 mM NaCl, 500 mM Imidazole, pH 8.0) and then followed by PD-10 desalting column (Amercham Pharmasia Biotech., NJ, USA).

## 3. Isolation of PLC isozymes from rat heart tissue

Tissue was homogenized in five volumes of homogenization buffer (10 mM Tris–HCl buffer [pH 7.4] containing 1 mM EDTA, 1 mM EGTA, 1 mM DTT, 1 mM PMSF, 10 mg/mL leupeptin, 10 mg/mL aprotinin, and calpain inhibitors I and II [each at 4 mg/mL]), and then the homogenate was

centrifuged at 100,000x$g$ for 1 h. The supernatant was adjusted to 2 M KCl by the addition of solid KCl, stirred for 2 h at 4 °C, and then centrifuged at 35,000×$g$ for 30 min. The resulting supernatant was dialyzed overnight against 4 L of homogenization buffer and re-centrifuged. The supernatant (∼80 mg of protein) was applied to a heparin–sepharose CL-6B column (20 mL of gel packed in a 1.5 cm×15 cm Econo column) that had been equilibrated with 20 mM HEPES-NaOH (pH 7.0) containing 1 mM EGTA and 0.1 mM DTT. Bound proteins were eluted at a flow rate of 4 mL/min with equilibration buffer containing 1.2 M NaCl. Fractions (16 mL) were collected and assayed for PLC activity. Essentially all detectable PLC activity was eluted in six fractions (∼40 mg protein), which were pooled and concentrated in a stirred ultrafiltration cell fitted with a YM30 membrane (Amicon, Danvers, MA, USA). After the final salt concentration was adjusted to 50 mM NaCl, the concentrate was centrifuged at 100,000×$g$ for 10 min. Proteins (20 mg, unless otherwise indicated) from the supernatant were injected onto a TSK gel heparin-5PW HPLC column (7.5mm×75mm) that had been equilibrated with 20 mM HEPES-NaOH (pH 7.0), 1 mM EGTA, and 0.1 mM DTT. Proteins were eluted with equilibration buffer, at a flow rate of 1 mL/min for 15 min, followed by a stepwise linear NaCl gradient of 0-0.64 M

for 40 min and from 0.64 to 1 M NaCl for 10 min. The column was then washed with equilibration buffer containing 1 M NaCl. Fractions (0.5 mL) were collected and assayed for PLC activity (50 mL and 5 mL of each fraction were used to assay PI- and PIP$_2$-hydrolyzing activity, respectively).

## 4. PLC assay

PLC activity was determined using [$^3$H]-PI or [$^3$H]-PIP$_2$ as the substrate. PIP$_2$-hydrolyzing activity was determined with mixed lipid vesicles of phosphatidylethanolamine and PIP$_2$ in a molar ratio of 4:1. The lipids in chloroform were dried under a stream of nitrogen gas, resuspended in 50 mM HEPES–NaOH (pH 7.0), 120 mM KCl, 10 mM NaCl, and 1.6 mM sodium deoxycholate and sonicated. Assays were performed for 10 min at 30 ˚C in a 100 µL reaction mixture containing lipid micelles (12 µM [$^3$H]-PIP$_2$, 12,000 cpm), 50 mM HEPES-NaOH (pH 7.0), 0.1 % sodium deoxycholate, 120 mM KCl, 10 mM NaCl, 2 mM MgCl$_2$, 2 mM EGTA, and 1.4 mM CaCl$_2$ (to give a final free Ca$^{2+}$ concentration of 1 mM). PI-hydrolyzing activity was measured in a 200 µL reaction mixture containing 150 mM [$^3$H]-PI (20,000 cpm), 50 mM HEPES-NaOH (pH 7.0), 3 mM CaCl$_2$, 2 mM EGTA, and 0.1% sodium deoxycholate. The reaction mixture was incubated at 37 ˚C for 10 min.

Reactions were terminated with a mixture of chloroform, methanol, and HCl, and $^3$H radioactivity in the aqueous phase was determined as described previously [57].

**5. Transfection**

Transfection of PLCδ1 cloned into the eukaryotic expression vector pcDNA3.1-HA was performed using the LIPOFECTAMIN PLUS$^{TM}$ reagent (Gibco BRL, Paisley, UK) [48]. Briefly, neonatal rat cardiomyocytes cultured on a 60 mm culture plate ($5 \times 10^5$ cells/plate) were washed twice with serum-free α-MEM. The LIPOFECTAMIN PLUS$^{TM}$ reagent was diluted with serum-free α-MEM and combined with 5 mg of DNA for each plate. The DNA and LIPOFECTAMIN PLUS$^{TM}$ reagent were added to each plate containing cells on fresh medium. After incubation for 12 h in a $CO_2$ incubator at 37 ˚C, the medium was exchanged with 10 % FBS-α-MEM. The cells were further incubated for 48 h at 37 ˚C. For simulated ischemia, the cells transfected with PLCδ1 were treated with deoxygenated α-MEM containing 1 % FBS and then incubated in an anaerobic chamber.

**6．Myocardial ischemia/reperfusion protocol and treatment with Hph1-**

**PLCδ1**

The experiments were conducted in accordance with the international Guide for the Care and Use of Laboratory Animals. The experimental protocol was approved by the Animal Research Committee of the Yonsei University College of Medicine. The myocardial infarction animal model was created through the method of Lipsic et al. with minor modifications [58]. Under general anesthesia, male Sprague-Dawley rats (230 ± 10 g) of 8 weeks of age were ventilated with positive-pressure (180 mL/min) using a Harvard ventilator (Harvard Apparatus, Millis, MA, USA). The rat heart was exposed through a 2 cm left lateral costal rib incision. The proximal portion of the left coronary artery was ligated with a 6-0 silk suture (ETHICON Inc., Somerville, NJ, USA) placed beneath the left atrium for 1 h. After occlusion, the ligature was removed for reperfusion. Successful reperfusion was indicated by the restoration of redness. The skin was sutured and the thorax was closed under negative pressure. Hph1-PLCδ1 was intravenously injected at the time of reperfusion.

**7. Hypoxia/reoxygenation injury and treatment with Hph1-PLCδ1**

Cardiomyocytes were incubated in 5 % $CO_2$ at 37 °C, and then the medium, on which the cells were growing, was exchanged with deoxygenated α-MEM (Gibco BRL, Paisley, UK) without FBS in anaerobic chamber (Thermo Forma Anaerobic System Model 1025, Marietta, USA). After incubation for 12 h, reperfusion was carried out with 10 % α-MEM maintained in 5 % $CO^2$ at 37 °C for 1 h. Hph1-PLCδ1 (0.1 µM and 0.5 µM) was pretreated before reperfusion.

## 8. Measurement of intracellular reactive oxygen species generation

Neonatal rat cardiomyocytes were labeled with 2′,7′-dichlorodihydro-fluorescein diacetate ($H_2$DCFDA; Molecular Probe, CA, USA). The probe $H_2$DCFDA (10µM) enters the cell, and the acetate group on $H_2$DCFDA is cleaved by cellular esterases, trapping the nonfluorescent 2′,7′-dichloro-fluorescin (DCFH) inside. Subsequent oxidation by reactive oxygen species yields the fluorescent product DCF. The dye, when exposed to an excitation wavelength of 480 nm, emits light at 535 nm only when it has been oxidized. Labeled cells were examined using a luminescence spectrophotometer for the oxidized dye.

## 9. Confocal microscopy and fluorescence measurements

The measurement of the cytosolic free $Ca^{2+}$ concentration was estimated by the confocal microscopy analysis. Neonatal rat cardiomyocytes were plated on a four-well slide chamber coated with 1.5 % gelatin for one day in α-MEM containing 10 % FBS (Gibco BRL, Paisley, UK) and 0.1 µM BrdU (Sigma Chemical St., Louis, MO, USA). After incubation, the cells were washed with modified Tyrode's solution with 0.265 g/L $CaCl_2$, 0.214 g/L $MgCl_2$, 0.2 g/L KCl, 8.0 g/L NaCl, 1.0 g/L glucose, 0.05 g/L $NaH_2PO_4$, and 1.0 g/L $NaHCO_3$. Cells were then loaded with 10 µM of the acetoxymethyl ester of fluo-4 (Fluo-4 AM, Molecular Probes, CA, USA) for 20 min, in the dark at 37 °C. Fluorescence images were collected using a confocal microscope (Leica, Solms, Germany) by excitation with a 488 nm line of argon laser, and emitted light was collected through a 510-560 nm band-pass filter. Relative data of intracellular $Ca^{2+}$ was determined by measuring the intensity of the fluorescence.

## 10. Determination of cell viability (proliferation assay)

Cardiomyocytes were plated in triplicate wells of 96-well plates at a density of

19

$1 \times 10^5$,and pretreated with Hph1-PLCδ1 for 30 min prior to exposure to hypoxia. Cell viability was determined by the MTT assay. After the incubation period, 3-(4,5-Dimethylthiazol-2-yl)-2,5-diphenyltetrazolium bromide (MTT) solution (Sigma, MO, USA) was added to each well to a final concentration of 0.5 mg/mL and was incubated at 37 °C for 3 h to allow MTT reduction. The formazan crystals were dissolved by adding dimethylsulfoxide (DMSO), and absorbance was measured at the 570 nm with a spectrophotometer.

## 11. Measurement of mitochondrial membrane potential

To measure mitochondrial membrane potential ($\Delta\psi_m$), cardiomyocytes were exposed to hypoxia/reoxygenation (12 h/1 h). Cells were trypsinized, washed with PBS, and incubated with 5,5',6,6'-tetrachloro-1,1',3,3'-tetraethyl-benzamidazolocarbocyanine iodide (JC-1) (Immunochemistry Technologies, LLC) at 37 °C for 10 min in the dark. Flow cytometric analysis was performed on FACSCalibur system (Becton Dickinson, San Jose, CA, USA) using CellQuest™ software with 10,000 events recorded for each sample. JC-1 monomer (green) fluorescence was observed by excitation with the 488 nm laser and examination of the emissions at 530 nm. JC-1 aggregate (red) fluorescence was observed by examination of the emissions at 590 nm. Data

was acquired in single parameter histogram with appropriate particle size and light scatter gating.

## 12. ROS-induced mPTP opening in mitochondria

Opening of the mPTPs was measured by the modified Petronilli method [54]. Cells ($10^5$) were cultured for one day in a lumitrac 600 96-well plate (Greiner Bio-One, Kremsmünster, Austria) coated with 1.5 % gelatin. After attachment, Hph1-PLCδ1 was added to the cells for 30 min before calcein loading. Cells were washed twice with Dulbecco's phosphate-buffered saline (cat # 14287, Gibco BRL, Paisley, UK) and 1 µM calcein-AM (Molecular Probe, Eugene, OR, USA). Membrane-permeant ester form was loaded for 10 min. To quench the cytosolic and nuclear calcein fluorescence, 1 mM $CoCl_2$ was, additionally, loaded for 15 min. Cells were washed with Dulbecco's PBS and 10 µM cyclosporine A (CsA), an mPTP opening inhibitor, and incubated for 30 min. Following a 500 µM $H_2O_2$ treatment, calcein fluorescence was measured on a Perkin-Elmer LS5 fluorescence spectrophotometer at 488 nm for excitation and 520 nm for emission. When calcein was released into the cytosol through mPTP opening, which was stimulated by the $H_2O_2$, cytosolic calcein was quenched by $CoCl_2$ and lower fluorescence intensity was detected.

## 13. Cell fractionation and western blotting

To quantify cytochrome C release, analysis of mitochondrial and cytosolic protein fractionation was performed. After the $5 \times 10^6$ cardiomyocytes were harvested, the cell pellets were resuspended with 100 µl of buffer (20 mM Hepes, pH 7.5, 1.5 mM $MgCl_2$, 10 mM KCl, 1 mM EDTA, 1mM E GTA, 250 mM sucrose, 0.1 mM PMSF, 1 mM dithiothreitol, 4 µg/ml pepstatin, 4 µg/ml leupeptin, 5 µg/ml aprotinin). After incubation on ice for 10 min , the cells were centrifuged at 750x$g$ for 10 min at 4 °C, and the supernatant was further centrifuged at 10,000x$g$ for 30 min at 4 °C. The mitochondrial pellets were resuspended in buffer, and the supernatant (cytosolic protein) was saved for western blot and caspase 3 assays. The protein concentration of each fraction was determined by BCA (Pierce Biotechnology, Rockford, IL, USA). Proteins were separated by SDS-PAGE using 12-15 % polyacrylamide gels and then electrotransferred to methanol-treated polyvinylidene difluoride membranes. The blotted membranes were washed twice with water and blocked by incubation with 10 % nonfat dried milk in PBS buffer (8.0 g NaCl, 0.2 g KCl, 1.5 g $NaH_2PO_4$, 0.2 g $K_2HPO_4$ per liter). The membranes were probed with anti-cytochrome C (Santa Cruz Biotechnology, Inc., CA, USA), anti-Bcl2

(Santa Cruz Biotechnology, CA, USA), and anti-Bax (Stressgen Biotechnologies, BC, Canada) followed by goat anti-mouse and goat anti-rabbit IgG-peroxidase. The blots were detected using enhanced chemi-luminescence kits (ECL, Amersham Pharmacia Biotech, Piscataway, NJ, USA).

## 14. Measurement of caspase 3 activity

Relative caspase 3 activity was determined using ApopTarget[TM] Caspase 3 Colorimetric Protease Assay, according to the manufacturer's instructions (Biosource, London, UK). This assay is based on the generation of free DEVD-*p*NA chromophores when the provided substrate is cleaved by caspase 3. Upon cleavage of the substrate by caspase 3, free *p*NA light absorbance can be quantified using a microplate reader at 405 nm. Briefly, the cultured neonatal cardiomyocytes ($2 \times 10^6$), after different treatments, were harvested in lysis buffer (1 M DTT), and cell extracts were centrifuged to eliminate cellular debris. Aliquots (50 µL) of the cell extracts were incubated at 37 °C for 2 h in the presence of the chromophore substrate. Free DEVD-*p*NA was determined colorimetrically. The comparison of absorbance of *p*NA from the apoptotic sample with uninduced control allows determination of the fold

increase in caspase 3 activity.

## 15. RT-PCR analysis

Total RNA was prepared using a Ultraspect™-II RNA system (Biotecx Laboratories, USA), and single-stranded cDNA was then synthesized from isolated total RNA using avian myeloblastosis virus (AMV) reverse transcriptase. A 20 μL reverse transcription reaction mixture containing 1 μg of total RNA, reverse transcription buffer (10 mM Tris–HCl, pH 9.0, 50 mM KCl, 0.1% Triton X-100), 1 mM deoxynucleoside triphosphates (dNTPs), 0.5 units of RNase inhibitor, 0.5 μg of oligo(dT)$_{15}$, and 15 units of AMV reverse transcriptase were incubated at 42 °C for 15 min, heated at 99 °C for 5 min, and then incubated at 0-5 °C for 5 min. PCR was performed for 35 cycles with 3′ and 5′ primers based on the sequences of the ryanodine receptor 2 gene primer (5'-CCAACATGCCAGACCCTACT-3' and 5'-TTTCTCCAT-CCTCTCCCTCA-3') and the $Na^+$-$Ca^{2+}$ exchanger 1 gene primer (5'-TGTCTGCGATTGCTTGTCTC-3' and 5'-TCACTCATCTCCACCAGACG-3'). The GAPDH primers (5'-CTCCCAACGTGTCTGTTGTG-3' and 5'-TGAGCTTGACAA- AGTGGTCG-3') were used as the internal standard. The signal intensity of the amplification product was normalized to its respective

GADPH signal intensity.

## 16. Determination of myocardial infarct size (area of fibrosis)

To measure infarct size, the rat heart was visualized through the intercostal space and excised. It was perfused with phosphate buffered saline (Gibco BRL, Paisley, UK) to remove the blood. The perfused heart was fixed in 10% formalin solution (Sigma Chemical St., MO, USA) for 24 h at 4 °C. Then, the heart was embedded in a paraffin block, and a 2 µm slides were prepared using Masson's trichrome stain. The total infarct size was measured with MetaMorph software version 4.6 (Universal Imaging Corp.) in the control (n=6), MI+saline (n=6), and MI+Hph1-PLCδ1 (n=6) groups. The infarct size was expressed as a percentage of the total left ventricle (LV).

## 17. Hematoxylin and eosin (H&E) staining

The paraffin block was made and 2 µm slides were stained with H&E. To observe the thickening of the wall of the LV, ten different LV wall regions per section were measured and averaged.

## 18. Terminal Deoxynucleotidyl Transferase–Mediated dUTP Nick-End

**Labeling (TUNEL) Assay**

The TUNEL Assay was performed according to the instructions of the manufacturer (Chemicon, CA, USA). In brief, the excised heart tissue was fixed in 10 % buffered formaldehyde and embedded in paraffin. Tissue sections, 5 μm thick, were deparaffinized, rehydrated, and rinsed with PBS. A positive control sample was prepared from normal heart tissue by treating with DNase I (10 U/ml, 10 min at room temperature). The sections were pretreated with 3.0 % $H_2O_2$, subjected to the reaction with the TdT enzyme for 37 °C for 1 h, and incubated with a digoxigenin-conjugated nucleotide substrate at 37 °C for 30 min. The nuclei exhibiting DNA fragmentation were shown by staining with 3,3-diaminobenzidine (DAB) (Vector Laboratories, CA, USA) for 5 min; the nuclei of apoptotic cardiomyocytes stained dark brown. Lastly, the sections were counterstained with methyl green, and a cover slip was applied. The sections were observed by light microscopy. Six slices per group were prepared, and ten different regions were observed in each slice (×200).

**19. Rat echocardiography**

The rats were sedated with zoletil (50 mg/kg) and xylazine (5 mg/kg), both of which were given intraperitoneally. Imaging was performed at 15 MHz with a linear transducer interfaced with an ultrasound system (Vivid 7, GE Vingmed Ultrasound, Horten, Norway). Two-dimensional guided M-mode and two-dimensional echocardiographic studies were performed at the mid-papillary muscle level, and all data were recorded and, subsequently, analyzed at the end of the study. For each animal, the LV end-systolic dimensions (LVESD) and LV end-diastolic dimensions (LVEDD) were measured from the M-mode tracings, and the LV shortening fraction (FS), ejection fraction (EF), end-systolic circumferential strain (S circ), and radial strain (S rad) were calculated.

## 20. Image analysis

Quantitative image analysis was performed with image analysis software (ImageJ).

## 21. Statistical analysis

Data are expressed as means±SEM. Student's t-test was used to compare two groups, and examination of more than two groups was done by one-way

ANOVA, using the Bonferroni test. A $p$-value <0.05 was considered significant.

## III. RESULTS

## 1. Cardioprotective role of PLCδ1 in hypoxia and ischemia

### 1.1 Changes of cardiac PLC isozymes in infarcted heart tissue

The amounts and activities of PLC isozymes were estimated by immunoblotting and identification of PI-hydrolyzing activity in the normal rat heart. Three main PLC activity peaks were identified. PLCδ1 activity was three times that of the other isozymes, PLCβ1 and PLCγ1 (Fig.1A). The amount of PLCδ1 was estimated to be approximately 44 ng/mg of rat heart, and the amounts of PLCβ1 and PLCγ1 were 0.4 ng/mg and 6.8 ng/mg, respectively (Fig.1B). To examine changes in the levels of the PLC isozymes in the ischemic rat heart, PLC isozyme levels were determined in the infracted region, in the border region, and in normal tissue by immunoblot analysis. Infracted heart was characterized by TTC staining. After one day of coronary artery occlusion, expression of PLCδ1 was selectively degraded in both scar and border zone tissue, whereas PLCβ1 and PLCγ1 were not (Fig.2). These results indicate that PLCδ1 degradation may be related to cell death in ischemia.

**A**

δ1

γ1

β1

PLC activity (cpm)

PIP₂
PI

Retention time (min)

**B**

| Amounts of PLC isozymes in normal rat heart | | |
|---|---|---|
| PLC-β1 | PLC-γ1 | PLC-δ1 |
| | (ng/mg of total protein) | |
| 0.4 | 6.8 | 44 |
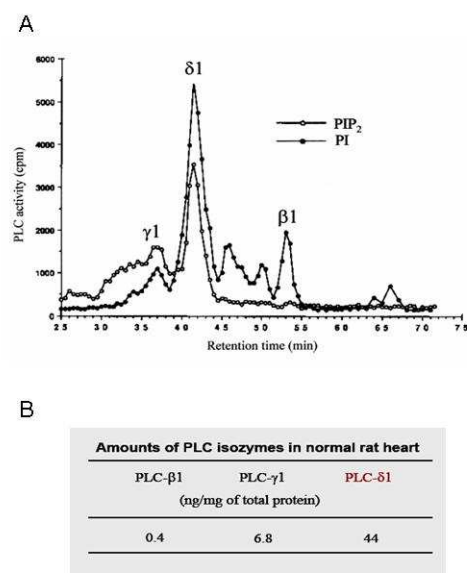
**Figure 1. Analysis of PLC isozymes in normal rat heart.** (A) The pooled PLC fraction from the heparin–sepharose chromatography was resolved by TSK gelheparin-5PW HPLC. Fractions (0.1 mL) were collected and assayed for both PI and $PIP_2$ hydrolysis. (B) Amounts of PLC isozymes in KCl extracts were directly calculated by quantitative immunoblotting of PLC standard.
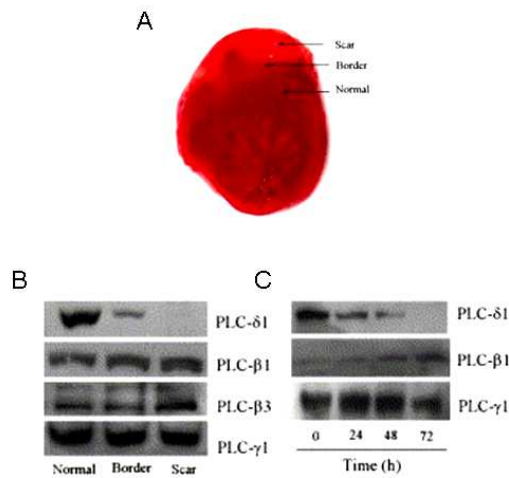
**Figure 2. Change in cardiac PLC isozymes in ischemic heart and cardiomyocytes.** (A) Photograph of a heart slice stained with triphenyl-tetrazolium chloride. (B) Representative western blots of PLC isozymes from normal, border, and scar regions of infarcted heart. Myocardial infarction was produced in Sprague–Dawley rats by surgical occlusion of the left coronary artery for 72 h before sampling the tissue. (C) PLC isozymes in hypoxic neonatal cardiomyocytes. Confluent neonatal cardiomyocytes (approximately $7 \times 10^6/10$ cm diameter dish) were subjected to hypoxia (N2:CO2:H2=85:10:5) in α-MEM containing 1 % FBS for the times indicated.

**1.2 Effect of calpain and/or caspase inhibitors on hypoxia-induced PLCδ1 degradation**

To confirm whether PLCδ1 degradation relates to proteases activated by increased intracellular $Ca^{2+}$ in hypoxia, neonatal cardiomyocytes were separately treated with 100 nM calpastatin, a calpain inhibitor, and 10 mM zVAD-fmk, a caspase pseudosubstrate inhibitor. Both inhibitors prevented the degradation of PLCδ1 in hypoxic neonatal cardiomyocytes (Fig. 3).
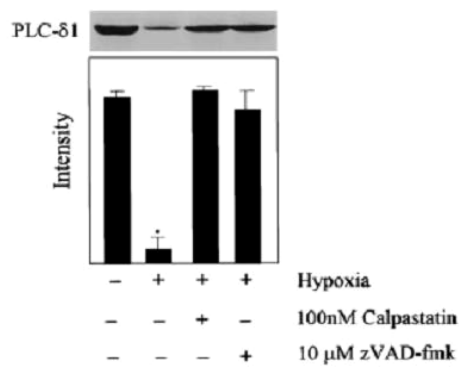
**Figure 3. Effect of protease inhibitors on PLCδ1 degradation in hypoxic neonatal cardiomyocytes.** Confluent neonatal cardiomyocytes (approximately $7 \times 10^6$/10 cm diameter dish) were subjected to hypoxia in α-MEM with no serum for 48 h. Calpastatin (100 nM) or zVAD-fmk (10 mM) was added into the medium. Figures show a representative western blot and relative intensity of PLCδ1 for three separate experiments. The mean±SEM of three independent experiments is reported. *$p$<0.05 vs. control.

## 1.3 Role of PLCδ1 on the cytosolic $Ca^{2+}$ overload by hypoxic conditions

Ischemia causes $Ca^{2+}$ overload in the cardiomyocytes. To address the role of PLCδ1 in $Ca^{2+}$ homeostasis in ischemic conditions, the PLCδ1 gene was cloned into pcDNA3.1-HA and was transfected into in neonatal cardiomyocytes. The cells overexpressing PLCδ1 were put in an anaerobic chamber. The hypoxic cells showed a significant increase in fluorescence intensity, indicating $Ca^{2+}$ overload. However, the hypoxic cells overexpressing PLCδ1 that were treated with calpastatin, a calpain inhibitor, showed normal fluorescence intensity, relative to the controls (pcDNA3.1-HA vector only). The increase in PLCδ1 expression by gene transfection and inhibition of PLCδ1 degradation by calpastatin treatment were examined by western blotting (Fig.4).
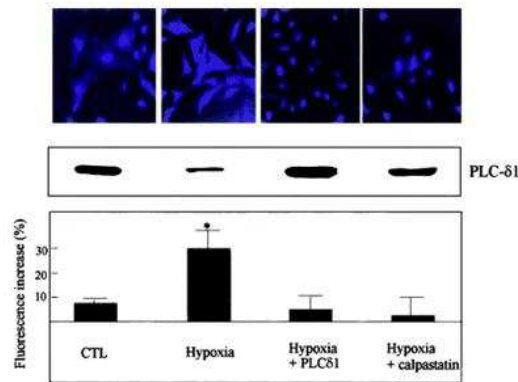
**Figure 4. Effect of PLCδ1 on intracellular Ca²⁺ concentration.** Confocal
fluorescent images of neonatal rat cardiomyocytes were obtained by loading
with flou-4 AM. The cells with pcDNA3.1-HA (CTL) or pcDNA3.1-HA +
PLCδ1 were incubated in an anaerobic chamber for 24 h. Mean increases of
the normalized fluorescence level in individual cells were observed in the
each condition. The mean±SEM of eight independent experiments is reported.
*$p<0.05$ vs. control.

## 1.4 Transduction of Hph1-PLCδ1 fusion proteins into cardiomyocytes

To introduce PLCδ1 more effectively into the cardiomyocytes, protein transduction domains (PTDs), YARVRRRGPRR, were used (Fig.5A). To analyze the transduction ability of Hph1-PLCδ1 fusion proteins into cardiomyocytes, Hph1-PLCδ1 was introduced into the cardiomyocytes in a dose-dependent and time-dependent manner. Hph1-PLCδ1 (0.1-0.5 µM) was detected by concentration (Fig.5B). PLCδ1 was first detected at 5 min, and the maximum intracellular concentration was reached in less than 15 min. In addition, PLCδ1 was maintained for more than 12 h in cardiomyocytes (Fig.5C).
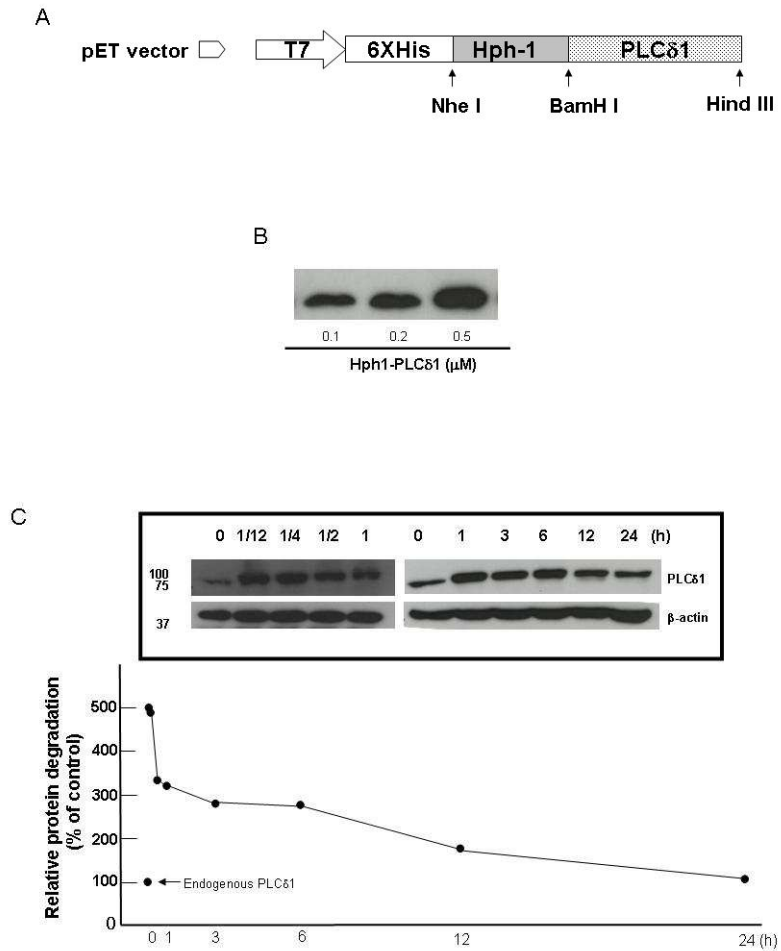
**Figure 5. Construction, transduction activity, and kinetics of the Hph1-PLCδ1 fusion protein in cardiomyocytes.** (A) Structure of the Hph1-PLCδ1 conjugated fusion proteins (B) Hph1-PLCδ1 (0.1-0.5 µM) was incubated in

α-MEM with 1 % FBS for 1 h and (C) 0.1 µM Hph1-PLCδ1 was incubated in α-MEM with 1 % FBS and then collected during 24 h. PLCδ1 was detected by western blotting and analyzed.

**1.5 Rescue of Ca$^{2+}$ overload by Hph1-PLCδ1 in hypoxic cardiomyocytes**

To identify whether the Hph1-PLCδ1 levels are maintained during 12 h of hypoxia, Hph1-PLCδ1 was pretreated in a concentration-dependent manner. PLCδ1 (0.1-0.5 µM) concentration was maintained during the 12 h of hypoxia (Fig.6A). As a previous study confirmed that PLCδ1 was selectively degraded in hypoxic cardiomyocytes and ischemic heart tissue, PLCδ1 (0.1-0.5 µM) was administered to hypoxic cardiomyocytes to aid in understanding its influence on cell survival. PLCδ1 prevented cell death in a concentration-dependent manner (Fig.6B), and the intracellular Ca$^{2+}$ level was significantly reduced by treatment with 0.1 µM Hph1-PLCδ1. The intracellular Ca$^{2+}$ concentration in hypoxic cells without PLCδ1 was about 1.5-fold higher compared to the controls, but hypoxic cardiomyocytes with PLCδ1 showed Ca$^{2+}$ levels similar to the controls (Fig.7).
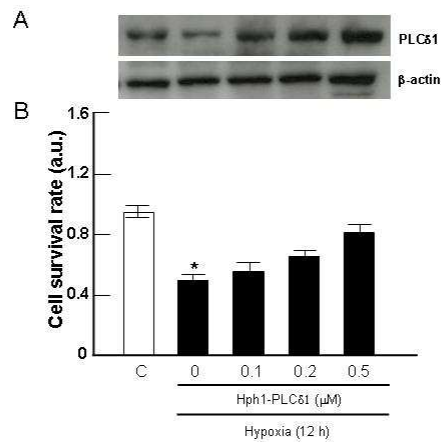
**Figure 6. Effect of the Hph1-PLCδ1 on cell death during hypoxia.**
Cardiomyocytes were incubated in the absence or presence of PLCδ1 (0.1-0.5 µM) under hypoxia for 12 h. (A) Endogenous and exogenous PLCδ1 were detected by western blotting. (B) Cell survival rate was detected by MTT assay and with the increased concentration of PLCδ1, cell death was inhibited. Each bar came from six wells of 96-well plate and represented the mean±SEM. *$p<0.05$ vs. control.
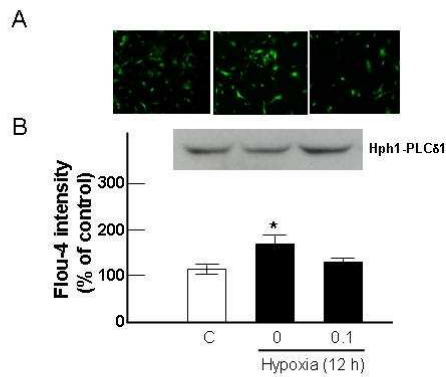
**Figure 7. Effects of Hph1-PLCδ1 on intracellular Ca²⁺ levels in cardiomyocytes.** (A) Representative fluorescence images represent cells in normal growth media, incubated in anaerobic media in the absence or presence of 0.1 μM PLCδ1. (B) Endogenous and exogenous PLCδ1 were detected by western blotting. The changes in fluorescence intensities, indicating intracellular Ca²⁺, were recorded by laser scanning confocal microscopy and were quantified in different cells (n=10) under differential conditions. *$p<0.05$ vs. control.

## 2. Cardioprotective role of PLCδ1 in hypoxia/reoxygenation and ischemia/reperfusion

## 2.1 Reactive oxygen species (ROS) production in hypoxic/reoxygenated cardiomyocyte

To show ROS production in hypoxic/reoxygenated (H/R) myocardium as compared with ischemic/reperfused (I/R) myocardium, ROS production was monitored at different times of the reoxygenation/reperfusion process in the cardiomyocytes. Exogenously added $H_2O_2$ was chosen as the positive control to compare the increase of intracellular ROS in reoxygenation/reperfusion. ROS production increased by 15 % with $H_2O_2$ (500 μM) treatment for 15 min in cardiomyocytes (Fig.8A). H (12 h)/R (1 h), also, caused a marginal increase in DCF fluorescence over the labeled normoxic control and hypoxic control cells (Fig.8B). These data indicate that H (12 h)/R (1 h) leads to meaningful ROS production.
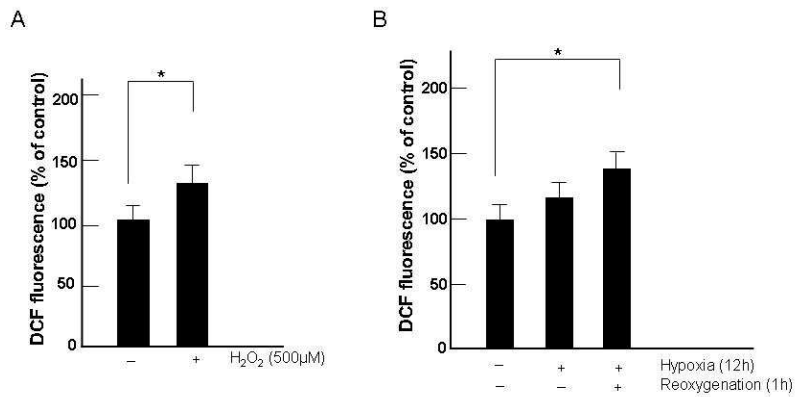
**Figure 8. Reactive oxygen species (ROS) production.** (A) 500 µM $H_2O_2$ as a positive control was added exogenously for 15 min (B) Cardiomyocytes were incubated with or without reperfusion for 1 h. Then ROS was assessed by DCF. The mean±SEM of three independent experiments is reported. *$p<0.05$ vs. control.

## 2.2 Rescue of $Ca^{2+}$ overload by Hph1-PLCδ1 in hypoxic/reoxygenated cardiomyocytes

Altered $Ca^{2+}$ homeostasis and ROS production play important roles in hypoxia/reoxygenation-induced cardiomyocyte injury [68, 69]. To know whether PLCδ1 treatment during reoxygenation decreased intracellular $Ca^{2+}$ overload, the intracellular $Ca^{2+}$ level was examined with using fluo-4 AM. A two-fold increase in fluorescence intensity, which correlates with the level of intracellular $Ca^{2+}$, was shown in the H/R cardiomyocytes, but intracellular $Ca^{2+}$ overload was significantly reduced by treatment with 0.1 µM Hph1-PLCδ1 (Fig.9).
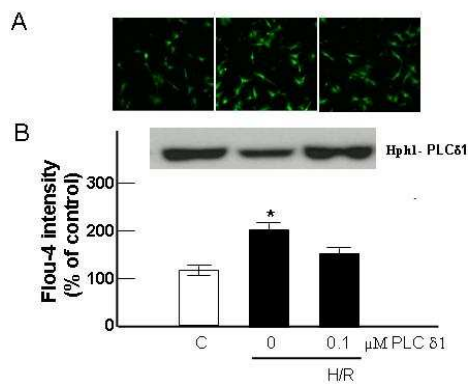
**Figure 9. Intracellular Ca²⁺ overload in H/R cardiomyocytes.** Cardio-myocytes were incubated in H (12 h)/R (1 h) and 0.1 µM PLCδ1 was added in reoxygenation. (A) Fluorescence image was obtained by using fluo-4 AM and (B) fluorescence intensity was quantified in different cells (n=10) in each condition and analyzed. Endogenous and exogenous PLCδ1 were detected by western blotting. *$p$<0.05 vs. control.

## 2.3 Mitochondrial permeability transition and membrane potential

To examine the relationship between PLCδ1 and apoptosis via opening of the mitochondrial permeability transition pores (mPTP), a high level of $H_2O_2$ (200-2000 µM) was administered to induce mPTP opening in cardiomyocytes. The opening of the mPTPs was calculated by estimating the amount of the remaining calcein-AM in the mitochondria. Calcein-AM was used to estimate the mPTP opening; 500 µM $H_2O_2$ induced the opening of 30 % of the mPTPs (Fig.10A). Pretreatment with 0.1 µM and 0.5 µM PLCδ1 caused a reduction of mPTP opening when the cells were exposed to $H_2O_2$ (500 µM, 15 min). Cyclosporin A (CsA), an mPTP inhibitor, was used as a positive control. (Fig.10B). Because changes in mitochondrial function result from opening of the mPTPs and this correlates with the loss in mitochondrial membrane potential as apoptosis is initiated, changes in the mitochondrial membrane potential were able to be ascertained. The cardiomyocytes showed red-orange (FL1) mitochondrial staining by JC-1 in normal high membrane potentials under control conditions. In contrast, cardiomyocytes treated with H (12 h)/R (1 h) showed green fluorescence (FL2), indicating loss of mitochondrial membrane potential. Pretreatment with PLCδ1 (0.1 µM and 0.5 µM)

significantly inhibited the green fluorescence in mitochondria and, thus, prevented ROS-induced mPTP opening (Fig.11).
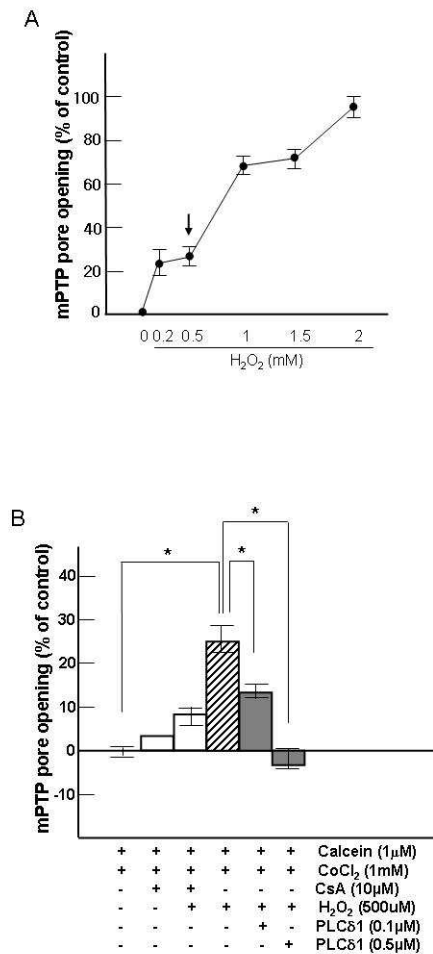


**Figure 10. PLCδ1 inhibits the release of mitochondrial calcein induced by opening of the mPTPs.** (A) mPTP opening was induced by $H_2O_2$ in a

concentration-dependent manner. Cardiomyocytes were cultured at 80 % confluence and treated with 200 to 2,000 µM $H_2O_2$, which corresponded to the induction of mPTP opening. (B) mPTP opening was induced by 500 µM $H_2O_2$ and calcein-AM fluorescence was assessed by fluorescence spectrophotometer. PLCδ1 was pre-incubated for 30 min. Each value is the mean±SEM of six independent experiments.
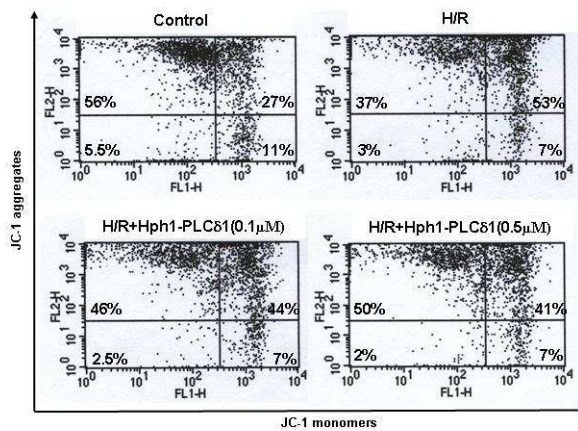
**Figure 11. Mitochondrial membrane potential was estimated by flow cytometry.** Cells were labeled with JC-1 for 15 min at 37 °C. H (12 h)/R (1 h) increased mitochondrial membrane depolarization (right upper panel), and PLCδ1 treatment inhibited this effect (right and left lower panel).

**2.4 PLCδ1 inhibits apoptosis through blocking of mPTP**

To examine whether PLCδ1, through inhibition of mPTP opening, inhibits apoptosis in reoxygenation, Bcl-2, Bax, cytochrome C release, and caspase 3 activation in H/R and H/R+PLCδ1 were examined. Although cytochrome C was released into the cytosol from the mitochondrial intermembrane space during H (12 h)/R (1 h), PLCδ1 treatment in reperfusion blocked cytochrome C release into the cytosol. PLCδ1 (0.1 µM and 0.5 µM) significantly inhibited Bax but restored Bcl-2 expression in whole cell lysates (Fig.12). Caspase 3 activity in cardiomyocytes undergoing H/R was significantly increased by 200 % relative to the control group (Fig.13). Treatment with PLCδ1 (0.1 µM and 0.5 µM) reduced the H/R-induced activation of caspase 3 to 159 % and 170 %, respectively.
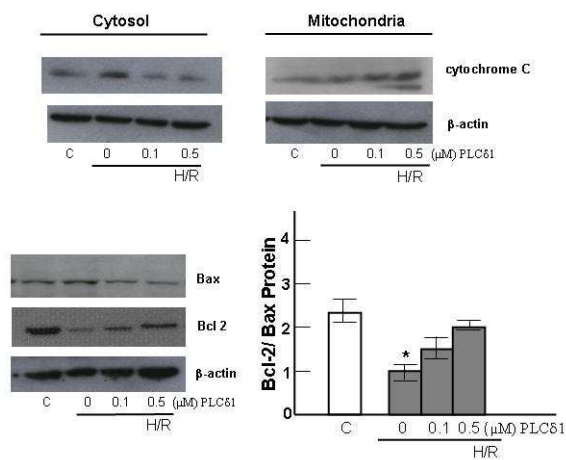
**Figure 12. Bcl-2/Bax ratio and cytochrome C release.** Cardiomyocytes were exposed to H (12 h)/R (1 h), and Hph1-PLCδ1 was added in reperfusion. Mitochondrial/cytosolic cytochrome C (top) and the Bcl-2/Bax protein ratio (bottom) were detected by western blotting. The mean±SEM of three independent experiments is reported. *$p < 0.05$ vs. control.
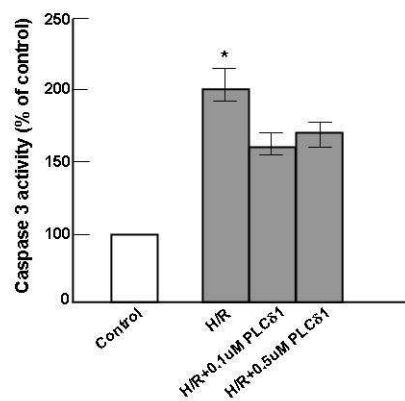
**Figure 13. Caspase 3 activity in cardiomyocytes.** Cells were exposed to H (12 h)/R (1 h) with or without Hph1-PLCδ1. The mean±SEM of three independent experiments is reported. *$p<0.05$ vs. control.

## 2.5 PLC$\delta$1 blocks intracellular calcium overload by hypoxic /reoxygenated cardiomyocytes

Previously, it was confirmed that PLC$\delta$1 regulates intracellular $Ca^{2+}$ overload via the inhibition of the release of ROS. To investigate whether PLC$\delta$1 regulates intracellular $Ca^{2+}$ concentration, which is important in cell function, changes in expression levels of one of the representative calcium channels in the T-tubule, the $Na^+$-$Ca^{2+}$ exchanger 1 (NCX1), and its receptor in the sarcoplasmic reticulum (SR) membrane, the Ryanodine Receptor 2 (RyR2), were tested in cardiomyocytes undergoing H/R. PLC$\delta$1 prevented changes in NCX1 and RyR2 expression levels in cardiomyocytes in H (12 h)/R (1 h) (Fig.14).
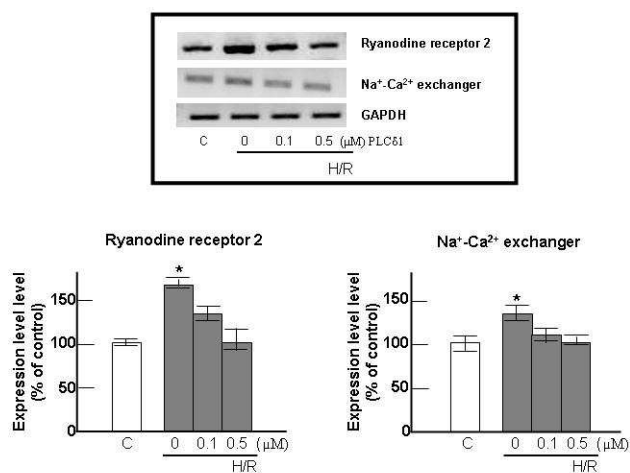
**Figure 14. PLCδ1 blocks changes in calcium channel expression in H/R.**
Expression levels of the ryanodine receptor (RyR) and the Na$^+$-Ca$^{2+}$ exchanger (NCX) were estimated in cardiomyocytes subjected to H (12 h)/R (1 h) with or without Hph1-PLCδ1 (top) and analyzed (bottom). Each value is the mean±SEM of three independent experiments. *$p<0.05$ vs. control.

## 2.6 Intravenous injection with Hph1-PLCδ1

PLCδ1 expression levels were examined in the normal heart region, reperfused heart region, and reperfused heart region that was injected with PLCδ1. The phosphorylation activity of the PKCs was detected as a marker that correlates with PLCδ1 activity. Hph1-PLCδ1 was injected intravenously with a final concentration of 36 nM. The rat heart tissue was isolated 3 h after injection to confirm delivery into the reperfused region. The level of PLCδ1 in the reperfused region of I/R and I/R+PLCδ1 groups was estimated by immunoblot analysis. PLCδ1 was significantly reduced in the I/R region in contrast to the control; however, PLCδ1 was restored in the same region by administration of Hph1-PLCδ1. Phosphorylation of the PKCs was decreased in the reperfused heart region, but this activity was restored by injection of Hph1-PLCδ1 (Fig.15).
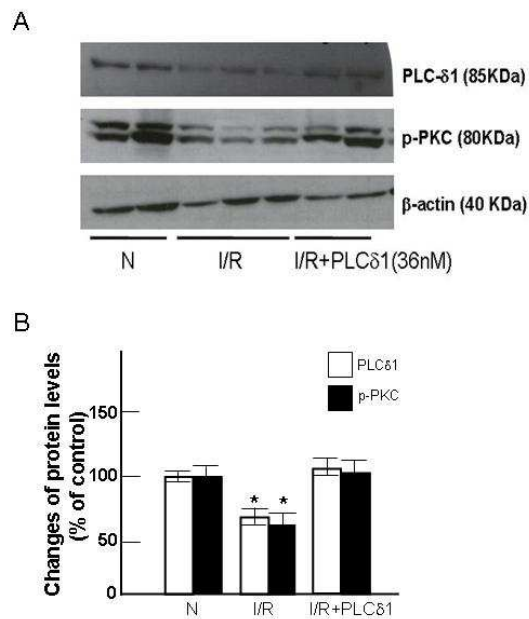
**Figure 15. Intravenous injection of 36 nM Hph1-PLCδ1 fusion protein.**
(A) PLCδ1 was detected 3 h after reperfusion in heart and (B) analyzed. Each value is the mean±SEM of three independent experiments. *$p<0.05$ vs. control.

## 2.7 PLCδ1 is cardiac protective in ischemia/reperfused heart

To investigate the therapeutic application of PLCδ1 *in vivo*, the experimental and control rats were sacrificed two weeks after reperfusion. Each rat heart was sectioned longitudinally. The left ventricular wall in the I/R rat heart was thinner than that of the control. Left ventricular wall thinning was reduced by PLCδ1 injection (Fig.16). In order to determine the percentage of interstitial fibrosis as a cardiac infarction index in the four groups, myocardial sections were stained with Masson's Trichrome. The untreated I/R hearts showed significant interstitial fibrosis (25±3 %) compared with the control hearts (1.2±0.5 %). PLCδ1 significantly decreased interstitial fibrosis to 7.5±4 % and 9±3.5 %, respectively (Fig.17). A TUNEL assay was used to identify the percentage of apoptotic cell in the cardiac tissue of the untreated I/R and PLCδ1-treated I/R groups. The incidence of TUNEL-positive myocardial cells caused by I/R was significantly reduced in the PLCδ1-treated I/R hearts compared with that of the I/R hearts (Fig.18). I/R-induced apoptosis in myocardial tissue was attenuated by PLCδ1 (36 nM and 108 nM) treatment.
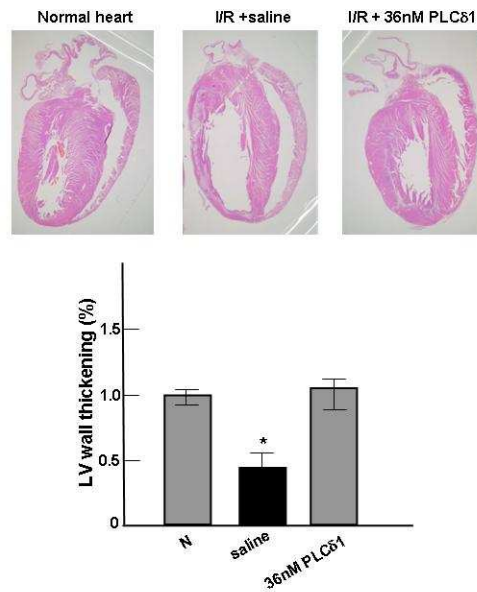
**Figure 16. Left ventricular wall thickening.** Hearts were sacrificed after I (1 h)/R (2 weeks). Representative hematoxylin and eosin staining images from histological sections (magnification: ×1.6) (top) and histogram show restored wall thickness in the I/R+36 nM Hph1-PLCδ1 group (bottom). Each value is the mean±SEM of six independent experiments. *$p$<0.05 vs. control.
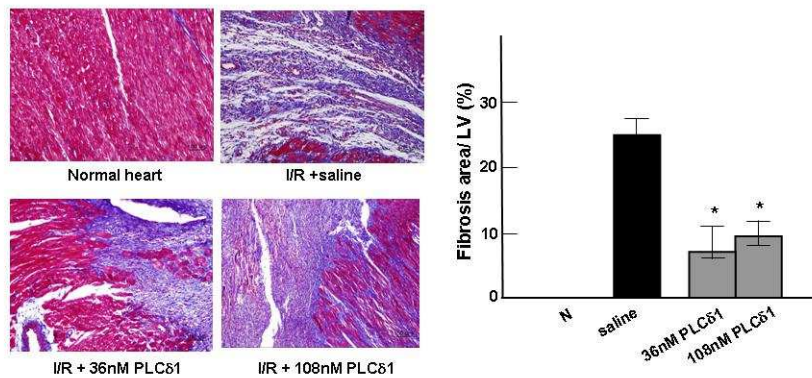
**Figure 17. Histological analysis of infarct rat hearts.** Hearts were sacrificed after I (1 h)/R (2 weeks). The left panel shows representative Masson's trichrome images from histological sections (magnification: ×200), and the right histogram shows less fibrosis (blue) in I/R+36 nM and 108 nM Hph1-PLCδ1 groups. Each value is the mean±SEM of six independent experiments. *$p<0.05$ vs. I/R+saline.
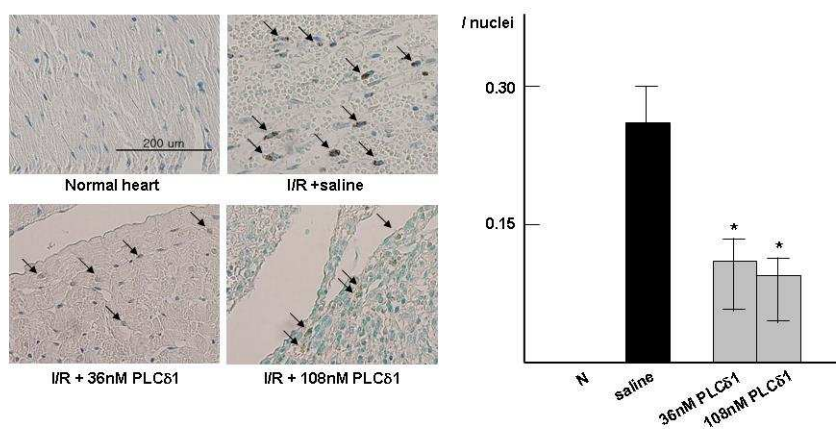
**Figure 18. Histochemical characterization of myocardial apoptosis.** The apoptosis assay was performed in heart tissue 2 weeks after reperfusion. The left panel shows representative images of TUNEL staining (magnification: ×200). Staining for normal nuclei (green) was carried out using methyl green, and apoptotic nuclei were stained brown. The right panel shows summarized data for the TUNEL staining. Each value is the mean±SEM of six independent experiments. *$p$<0.05 vs. I/R+saline.

## 2.8 Heart function studies

Heart function was estimated by echocardiographic analysis of the rat heart two weeks after reperfusion and the administration of therapeutics. There were three groups (n=6/group): control, I/R, and I/R+PLCδ1. The results from the echocardiographic examinations were compared between the control group and experimental animal groups. LV function and remodeling indices are summarized in Table 1. LV ejection fraction and LV fractional shortening in the I/R+PLCδ1 group were better that in the I/R group, but LV fractional shortening was not significantly better. The I/R group had much lower absolute values of radial strain (S rad) than the control group ($p<0.05$), and the I/R group had significantly higher values of circumferential strain (S cir) than the control group ($p<0.05$). S cir and S rad were improved by treatment with PLCδ1 in the I/R+PLCδ1 group relative to the I/R group ($p<0.05$) (Fig.19).

**Table 1. Echocardiography.**

| Variables | Control (n=6) | I/R (n=6) | I/R-PLCδ1 (n=6) |
|---|---|---|---|
| LVEDD, mm | 0.56±0.04 | 0.57±0.03 | 0.57±0.03 |
| LVESD, mm | 0.33±0.05 | 0.37±0.03 | 0.32±0.05 |
| FS, % | 41.39±0.04 | 35.94±4.17 | 43.69±8.38 |
| LVEDV, ml | 0.43±0.06 | 0.44±0.07 | 0.43±0.07 |
| LVESV, ml | 0.10±0.04 | 0.13±0.03 | 0.09±0.03 |
| LVEF, % | 76.49±6.14 | 71.50±5.61‡ | 79.78±7.40 |
| Peak S cir, % (infarct zone) | -20.16±5.54 | -7.84±4.06‡ | -17.11±6.57 ∬ |
| Peak S rad, % (infarct zone) | 48.33±10.02 | 22.02±8.92‡ | 40.62±11.44 ∬ |
| Global S cir, % | -20.32±6.42 | -12.40±4.93‡ | -21.66±5.95 ∬ |
| Global S rad, % | 45.23±8.42 | 34.41±6.58‡ | 43.42±7.62 ∬ |

Each value is given as mean±SEM. LVEDD=left ventricular end diastolic diameter, LVESD=left ventricular end systolic diameter, FS=fractional shortening, LVEDV=left ventricular end diastolic volume, LVESV=left ventricular end systolic volume, EF= ejection fraction, S cir=circumferential strain, S rad=radial strain. † $p < 0.01$ vs Control, ‡ $p < 0.05$ vs Control, ∫ p $< 0.01$ vs I/R, ∬ p $< 0.05$ vs I/R.
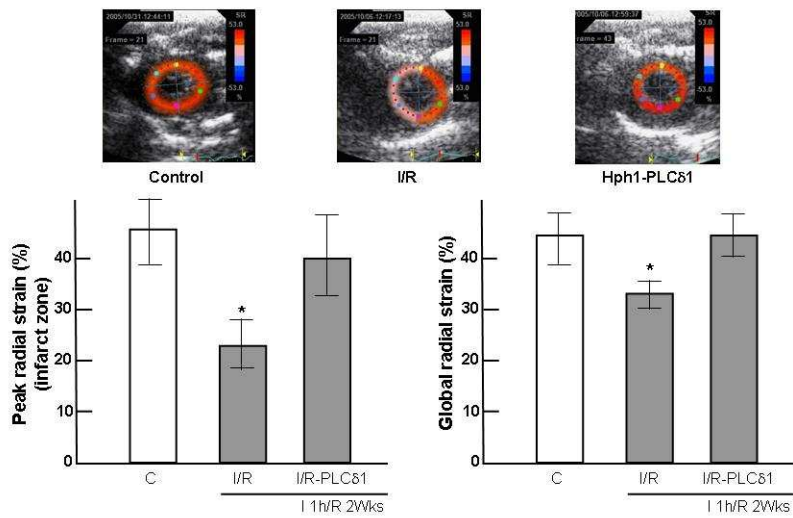
**Figure 19. Two-dimensional-echocardiography and two-dimensional-speckle-tracking imaging of left ventricle.** End-systolic radial strains show a loss of contraction in the infracted region (top). Colors show six different segments; anterior (yellow), lateral (cyan), posterior (green), inferior (magenta), septal (blue), and anteroseptal (red) walls. Reduced radial strains were improved by PLCδ1 administartion (bottom). Each value is the mean±SEM of the six independent experiments. *$p<0.05$ vs. control.

## IV. DISCUSSION

These results showed that the PLCδ1 protein decreased cell death through the reduction of the intracellular $Ca^{2+}$ overload induced by hypoxia. They, also, showed that PLCδ1 led to cell survival through regulation of mPTP opening and intracellular $Ca^{2+}$ regulatory proteins in hypoxia/reoxygenation (H/R). Ultimately, these actions inhibited apoptosis of cardiomyocytes *in vitro* and *in vivo*.

It was observed that intracellular $Ca^{2+}$ overload occurred with hypoxia and decreased with PLCδ1 gene transfection and PLCδ1 protein transduction (Fig.4 and Fig.7). Although myocardial apoptosis was related to the mitochondrial pathway-induced $Ca^{2+}$ overload in hypoxia [53], induction of mPTP opening has not been reported upon. It is thought that apoptosis in hypoxia may occurr independently of mPTP opening because other proteins, such as the $Ca^{2+}$ uniporter and $Na^+$-$Ca^{2+}$-exchanger, related to $Ca^{2+}$ influx and efflux exist in the mitochondrial membrane. Previously mentioned factors, besides low pH, could possibly be inhibiting mPTP opening in hypoxia [44].

A new method, which is a modification of Petronilli's methods, was used to detect mPTP opening. This modified method was useful in quantifying mPTP

opening in multiple conditions, without mitochondria isolation or image analysis [54, 55]. The protein transduction domain (PTD) Hph1 was used to rapidly and easily introduce PLCδ1 into the cardiomyocytes *in vitro* and *in vivo*. This study showed that Hph1-PLCδ1 was first detectable in cardiomyocytes within 5 min by western blotting (Fig.5). A fusion protein composed of Hph1 is a useful therapeutic tool in various disease models. Although the efficiency of Hph1 transduction into the cardiomyocytes was not examined in this study, Choi et al. reported that nearly 100% of the cells, including HeLa, HepG2, HaCat, and NIH3T3, were determined to be positive for enzymatic activity[70].

It is well known that reperfusion generates a burst of ROS. Significant ROS production was shown in reoxygenation, but little ROS production was shown in hypoxia; the latter was not significant (Fig.8). ROS generation in hypoxia has been reported by several researchers [62], and it was suggested as a possible reason that low oxygen presented, despite hypoxia, and generated ROS from mitochondria source [63]. Becker also showed that little ROS was detected in ischemia, but cell death was not meaningful relative to that of reperfusion [64].

*In vitro*, mPTP opening induced by the administration of 500 µM $H_2O_2$ was

estimated; mPTP opening was successfully inhibited by treatment with PLCδ1 (Fig.10B). However, the mPTPs opened in large numbers in response to treatment with high concentration $H_2O_2$ (2 mM) (Fig.10A), and PLCδ1 did not effectively inhibit mPTP opening (data not shown). These results suggest that it is advantageous to inject the PLCδ1 in early phase of reperfusion. This suggestion is supported by Becker's experiments. Becker demonstrated that ROS were increased within the first several minutes of reperfusion, and this was the time at which cell death occurred in large numbers [64]. To explain this large burst of ROS in reperfusion, Zorav et al. suggested the concept "ROS-induced ROS release" and demonstrated that ROS produced initially led to a large burst of ROS from the mitochondria of cardiomyocytes [65]. Jolly et al. reported that the protective effect of ROS scavengers was only significant they were administered prior to reperfusion, not after reperfusion [66]. Previously, many experiments have focused on the pretreatment with several drugs and materials *in vivo* and *in vitro* to cure diseases, but there were often many side effects. Therefore, the appropriate treatment time for PLCδ1 administration is considered very important.

As sustained opening of mPTP leads to disruption of the mitochondrial

membrane potential, $H_2O_2$ as a ROS production stimulus was administered to induce mPTP opening, and JC-1 was used to examine the mitochondrial membrane potential (Fig.11). Masaharu et al. demonstrated the relationship between mitochondrial membrane potential depolarization and mPTP opening in conditions of $H_2O_2$ administration by using TMRM and calcein in cardiomyocytes [67]. The restoration of mitochondrial membrane potential, as it relates to mitochondrial function, was further confirmed by using TMRM. PLCδ1 inhibited these changes in the mitochondrial membrane potential (data not shown).

Calcium ions play an important role in normal cardiac function, and several $Ca^{2+}$ regulating proteins are connected with $Ca^{2+}$ homeostasis in cardiomyocytes. In ischemia/reperfusion, SR function is depressed by decreased phosphorylation of the SR $Ca^{2+}$ handling proteins [69], and this event results in $Ca^{2+}$ overload, decreasing myocardial contractility [69, 70, 71]. Recent studies have shown that PLCδ1 reduces the level of intracellular $Ca^{2+}$ overload in I/R, an action which may closely relate to apoptosis [72, 73]. This result showed that RyR and NCX expression levels were increased by hypoxia/reoxygenation, and PLCδ1 blocked these changes in the levels of

expression (Fig.14). This means that PLCδ1 is involved in the regulation of intracellular $Ca^{2+}$ overload due to increased RyR and NCX expression. Yeung et al. showed that RyR and NCX expression was not changed in I/R and that activity was significantly increased during I/R in chronic intermittent hypoxia (CIH) [74]. On the other hand, many reports have demonstrated that variations in NCX and RyR expression were highly related to the regulation of intracellular $Ca^{2+}$ and heart function. Leszek et al. showed that NCX protein expression was increased in heart failure and had significant inverse correlations with LV diastolic and systolic indices [75]. Mishra et al. reported that increased NCX expression was clinically associated with the deterioration of LV function during the progression of heart failure [76]. In an experiment with cardiomyocytes from younger rats having a high expression of NCX, $Ca^{2+}$ uptake rates were significantly increased in $Na^+$ loading relative to sham cells [77]. Activation of RyR by ROS, by molecules such as $H_2O_2$ and $O^{2-}$, was demonstrated by several researchers [78, 79, 80].

PLCδ1 expression was observed and significantly reduced in the I/R heart relative to the control heart (Fig.15). Heart function was also decreased in the I/R heart (Fig.19). Tappia et al. showed that a defect in the PLCδ1 signaling

pathway, stimulated by phosphatidic acid (PA) in diabetic rat cardiomyocytes, may significantly contribute to heart dysfunction during diabetes and many different types of cardiac pathologies [45]. Lien et al. also demonstrated that PLCδ1 is critical for heart protection against adriamycin-induced cardiac injury by using transgenic mouse and microarray analysis [46]. PLCδ1 injected through the femoral vein was present in the reperfused heart region and maintained its biological activity. PLCδ1 activity was indirectly confirmed by estimating phosphorylation of protein kinase C (PKC). Degradation of PLCδ1 affected the activity of PKC; however, the activity was restored by PLCδ1 injection (Fig.15). Since PKC is a serine/threonine kinases, it has been implicated in a number of diseases, including ischemic heart disease and congestive heart failure [81]. Yigang and Muhammad reported that activation of PKC is associated with cardiac protection in I/R [82]. These results are consistent with cardiac survival following PKC activation in this study. Since PKC activation results in activation of PLCδ1, it was speculated that PLCδ1 may play important roles for cardiac survival in ischemia/reperfusion conditions.

*In vivo*, the cardioprotective effects of PLCδ1 were demonstrated by

histological staining and histochemistry. In hematoxylin and eosin (H&E) staining, decreased wall thickness of the left ventricle (LV) in I/R was improved with administration of PLCδ1 (I/R with PLCδ1) (Fig.16), and severe cellular damage in I/R was prevented with administration of PLCδ1 (Fig.18). Tang et al. demonstrated that infarct size and LV wall thickness are significantly related in MSC injected heart [83]. Interstitial fibrosis, as a histological marker, was used as an assessment of heart function (Fig.17). Fibrosis and collagen deposition were involved in the remodeling of failing myocardium by ROS release, and the phenotypic transformation of fibroblasts to myofibroblasts was associated with progression to end-stage heart failure [84].

In echocardiography, indices related to heart function were restored by PLCδ1 injection into the I/R heart (Table 1). Most notably, the parameters of S cir and S rad showed much improvement (Fig.19). Zora et al. demonstrated by using two-dimensional echocardiography that S cir and S rad were associated with segmental LV dysfunction following myocardial infarction and highly related to scar size and region [85]. These results coincide with present data.

In summary, these data indicate that a production of ROS and an increase in intracellular $Ca^{2+}$ levels by activated $Ca^{2+}$ regulatory proteins in H/R lead to

mitochondrial membrane transition and mPTP opening. This results in the release of cytochrome C (an intermembrane protein) and pro-apoptotic factors and activation of caspase 3. In turn, activation of $Ca^{2+}$-activated proteases leads to the degradation of PLCδ1, which, thereby, decreases PKC activation. Calcium homeostasis is not regulated in injured cardiomyocytes. Subsequently, myocardial apoptosis is initiated and heart function is impaired. Here, the amount of myocardium that was infarcted was reduced through the inhibition of mPTP opening by using the Hph1-PLCδ1 fusion protein *in vivo* and *in vitro*.

## V. CONCLUSION

This study showed, *in vitro,* that: 1) PLCδ1 reduced intracellular $Ca^{2+}$ overload by regulating $Ca^{2+}$-related channels in H/R; 2) PLCδ1 inhibited mitochondrial permeability transition pore (mPTP) opening induced by ROS and attenuated H/R-induced mitochondrial depolarization; and 3) as PLCδ1 inhibited increased cytosolic cytochrome C, changes in the Bcl-2 family protein levels, and caspase 3 activation by H/R, apoptosis was inhibited. It also showed that, *in vivo*: 1) reduced levels of PLCδ1 and PKC phosphorylation in reperfused heart tissue were restored through intravenous injection of Hph1-PLCδ1; 2) this resulted in the reduction of cardiac fibrosis and TUNEL positive-myocardial cells and then led to the improvement of heart function. The present data suggest that apoptosis of cardiomyocytes is inhibited by injection of PLCδ1 *in vitro* and *in vivo*. These are meaningful because PLCδ1, through application of the Hph1-PLCδ1 fusion protein, was used as not in a preventative, but therapeutic manner. Although this study demonstrates that PLCδ1 prevents myocardial apoptosis and heart dysfunction after reperfusion, the remodeling process after reperfusion involves a number of factors that may complexly influence cardiomyocyte apoptosis. Therefore,

further study should be undertaken to more completely understand the process

of cardiomyocyte remodeling.

**REFERENCES**

1. Maron BJ, Fananapazir L. Sudden cardiac death in hypertrophic cardiomyopathy. Circulation 1992;85:57-63.

2. Aboulhosn J, Child JS. Left ventricular outflow obstruction: subaortic stenosis, bicuspid aortic valve, supravalvar aortic stenosis, and coarctation of the aorta. Circulation 2006;114:2412-22.

3. Becker L, Ambrosio G. Myocardial consequences of reperfusion. Prog Cardiovasc Dis 1987; 30:23-44.

4. Lefer AM, Tsao PS, Lefer DJ, Ma XL. Role of endothelial dysfunction in the pathogenesis of reperfusion injury after myocardial ischemia. FASEB J 1991;5:2029-34.

5. McCord JM. Oxygen-derived free radicals in postischemic tissue injury. N Engl J Med 1985*;*312:159-63.

6. Li D, Shao Z, Vanden Hoek TL, Brorson JR. Reperfusion accelerates acute neuronal death induced by simulated ischemia. Exp Neurol 2007;206:280-7.

7. Mehran R, Dangas G, Abizaid A. Treatment of focal in-stent restenosis with balloon angioplasty alone versus stenting: Short- and long- term results. Am Heart J 2001;141:610-4.

8. Alfonso F, Zueco J, Cequier A. for the Restenosis Intra-stent: Balloon Angioplasty Versus Elective Stenting (RIBS) Investigators. A randomized comparison of repeat stenting with balloon angioplasty in patients with in-stent restenosis. J Am Coll Cardiol 2003;42:796-805.

9. Elezi S, Kastrati A, Hadamitzky M. Clinical and angiographic follow-up after balloon angioplasty with provisional stenting for coronary in-stent restenosis. Catheter Cardiovasc Intervent 1999;48:151-6.

10. Alfonso F, Cequier A, Zueco J. Stenting the stent: initial results and long term clinical and angiographic outcome of coronary stenting for patients with in-stent restenosis. Am J Cardiol 2000;65:327-32.

11. Thayssen P. Percutaneous transluminal coronary angioplasty in ischemic heart disease. Ugeskr Laeger 1994;156:4445-9.

12. Lee MS, Kapoor N, Jamal F, Czer L, Aragon J, Forrester J, et al. Comparison of coronary artery bypass surgery with percutaneous coronary intervention with drug-eluting stents for unprotected left main coronary artery disease. J Am Coll Cardiol 2006;21:878-81.

13. Fu XC, Wang MW, Li SP, Wang HL. Anti-apoptotic effect and the mechanism of orientin on ischaemic/reperfused myocardium. J Asian Nat Prod Res 2006;8:265-72.

14. Imahashi K, Schneider MD, Steenbergen C, Murphy E. Transgenic expression of Bcl-2 modulates energy metabolism, prevents cytosolic acidification during ischemia, and reduces ischemia/reperfusion injury. Circ Res 2004;95:734-41.

15. Argaud L, Gomez L, Gateau-Roesch O, Couture-Lepetit E, Loufouat J, Robert D, et al. Trimetazidine inhibits mitochondrial permeability transition pore opening and prevents lethal ischemia-reperfusion injury. J Mol Cell Cardiol 2005;39:893-9.

16. Li C, Jackson RM. Reactive species mechanisms of cellular hypoxia-reoxygenation injury. Am J Physiol Cell Physiol 2002;282:227-41.

17. Zhao ZQ, Velez DA, Wang NP, Hewan-Lowe KO, Nakamura M, Guyton RA, et al. Progressively developed myocardial apoptotic cell death during late phase of reperfusion. Apoptosis 2001;6:279-90.

18. Zhao ZQ, Morris CD, Budde JM, Wang NP. Inhibition of myocardial apoptosis reduces infarct size and improves regional contractile dysfunction during reperfusion. Cardiovasc Res 2003;59:132-42.

19. De Vries B, Matthijsen RA, Wolfs TG, van Bijnen AA, Heeringa P, Buurman WA. Inhibition of complement factor C5 protects against renal ischemia-reperfusion injury: inhibition of late apoptosis and inflammation. Transplantation 2003;75:375-82.

20. Moens AL, Claeys MJ, Timmermans JP, Vrints CJ. Myocardial ischemia/reperfusion-njury, a clinical view on a complex pathophysiological process. Int J Cardiol 2005;100:179-90.

21. Abbate A, Biondi-Zoccai GG, Baldi A. Pathophysiologic role of myocardial apoptosis in post-infarction left ventricular remodeling. J Cell Physiol 2002;193:145-53.

22. Rothstein EC, Byron KL, Reed RE, Fliegel L. H2O2-induced $Ca^{2+}$ overload in NRVM involves ERK1/2 MAP kinases: role for an NHE-1-dependent pathway. Am J Physiol Heart Circ Physiol 2002;283:598-605.

23. Waypa GB, Marks JD, Mack MM, Boriboun C. Mitochondrial reactive oxygen species trigger calcium increases during hypoxia in pulmonary arterial myocytes. Circ Res 2002;91:719-26.

24. Mukherjee SB, Das M, Sudhandiran G, Shaha C. Increase in cytosolic $Ca^{2+}$ levels through the activation of non-selective cation channels induced by oxidative stress causes mitochondrial depolarization leading to apoptosis-like death in Leishmania donovani promastigotes. J Biol Chem 2002;277:24717-27.

25. Pacher P, Csordas G, Hajnoczky G. Mitochondrial $Ca^{2+}$ signaling and cardiac apoptosis. Biol Signals Recept 2001;10:200-23.

26. Brookes PS, Yoon Y, Robotham JL, Anders MW, Sheu SS. Calcium, ATP, and ROS: a mitochondrial love-hate triangle. Am J Physiol Cell Physiol 2004;287:817–33.

27. Bolli R, Marbán E. Molecular and cellular mechanisms of myocardial stunning. Physiol Rev 1999;79:609-34.

28. Clanachan AS, Jaswal JS, Gandhi M, Bottorff DA. Effects of inhibition of myocardial extracellular-responsive kinase and p38 mitogen-activated protein kinase on mechanical function of rat hearts after prolonged hypothermic ischemia. Transplantation 2003;75:173-80.

29. Gao F, Yue T-L, Shi D-W, Christopher TA. p38 MAPK inhibition reduces myocardial reperfusion injury via inhibition of endothelial adhesion molecule expression and blockade of PMN accumulation. Cardiovasc Res 2002;53:414-22.

30. Cicconi S, Ventura N, Pastore D, Bonini P. Characterization of apoptosis signal transduction pathways in HL-5 cardiomyocytes exposed to ischemia/reperfusion oxidative stress model. J Cell Physiol 2003;195:27-37.

31. Wang T, Zhang X, Li J-J. The role of NF-κB in the regulation of cell stress responses. Int Immunopharmacol 2002;2:1509-20.

32. Crompton M. On the involvement of mitochondrial intermembrane junctional complexes in apoptosis. Curr Med Chem 2003;10:1473-84.

33. Gomez L, Thibault H, Gharib A, Dumont JM, Vuagniaux G, Scalfaro P, et al. Inhibition of mitochondrial permeability transition improves functional recovery and reduces mortality following acute myocardial infarction in mice. Am J Physiol Heart Circ Physiol 2007; 293:1654-61.

34. Townsend PA, Davidson SM, Clarke SJ, Khaliulin I, Carroll CJ, Scarabelli TM, et al. Urocortin prevents mitochondrial permeability transition in response to reperfusion injury indirectly by reducing oxidative stress. Am J Physiol Heart Circ Physiol 2007;293:928-38.

35. Shanmuganathan S, Hausenloy DJ, Duchen MR, Yellon DM. Mitochondrial permeability transition pore as a target for cardioprotection in the human heart. Am J Physiol Heart Circ Physiol 2005;289:237-42.

36. Basso E, Fante L, Fowlkes J, Petronilli V, Forte MA, Bernardi P. Properties of the permeability transition pore in mitochondria devoid of Cyclophilin D. J Biol Chem 2005;280:18558-61.

37. Zoratti M, Szabò I. The mitochondrial permeability transition. Biochim Biophys Acta 1995;1241:139-76.

38. Halestrap AP, Clarke SJ and Javadov1 SA. Javadov1 Mitochondrial permeability transition pore opening during myocardial reperfusion-a target for cardioprotection. Cardiovasc Res 2004;61:372-85.

39. Halestrap AP. The mitochondrial permeability transition: its molecular mechanism and role in reperfusion injury. Biochem Soc Symp 1999;66:181-203.

40. Tsujimoto Y, Shimizu S. Role of the mitochondrial membrane permeability transition in cell death. Apoptosis 2007;12:835-40.

41. Budd SL. Mechanisms of neuronal damage in brain hypoxia/ischemia: focus on the role of mitochondrial calcium accumulation. Pharmacol Ther 1998;80:203-29.

42. Hwang KC, Lim S, Kwon HM, Bae YS, Kang SM, Chung KH, et al. Phospholipase C-δ1 rescues intracellular $Ca^{2+}$ overload in ischemic heart

and hypoxic neonatal cardiomyocytes. J. Steroid Biochem. Mol Biol 2004;91:131-8.

43. Rebecchi MJ, Pentyala SN. Structure, function and control of phosphoinositide-specific phospholipase C. Physiol Rev 2000;80:1291-335.

44. Smith RJ, Justen JM, McNab AR. U-73122: a potent inhibitor of human polymorphonuclear neutrophil adhesion on biological surfaces and adhesion related effector functions. J Pharmacol Exp Ther 1996;278:320-9.

45. Tappia PS, Maddaford TG, Hurtado C, Dibrov E, Austria JA, Sahi N, et al. Defective phosphatidic acid-phospholipase C signaling in diabetic cardiomyopathy. Biochem Biophys Res Commun 2004;316:280-9.

46. Lien YC, Noel T, Liu H, Stromberg AJ, Chen KC, St Clair DK. Phospholipase C-delta1 is a critical target for tumor necrosis factor receptor-mediated protection against adriamycin-induced cardiac injury. Cancer Res 2006;66:4329-38.

47. Rhee SG, Bae YS. Regulation of phosphoinositide-specific phoapholipase C isozymes. J Biol Chem 1997;272:15045-8.

48. Lee KH, Lee NH, Lim SY, Jung HK, Kho YG, Park HY, et al. Calreticulin inhibits the MEK1,2-ERK1,2 pathway in a1-adrenergic receptor/Gh-stimulated hypertrophy of neonatal rat cardiomyocytes. J Steroid Biochem Mol Biol 2003;84:85-90.

49. Kintner DB, Luo J, Gerdts J, Ballard AJ, Shull GE, Sun D. Role of $Na^+$-$K^+$-Cl-cotransport and $Na^+/Ca^{2+}$ exchange in mitochondrial dysfunction in astrocytes following in vitro ischemia. Am J Physiol Cell Physiol 2007;292:1113-22.

50. Nakamura Y, Fukami K, Yu H, Takenaka K, Kataoka Y, Shirakata Y, et al. Phospholipase C delta1 is required for skin stem cell lineage commitment. EMBO J 2003;22:2981-91.

51. Schwarze SR, Alan H, Adamina VA and Dowdy SF. In vivo protein transduction: Delivery of a biologically active protein into the mouse. Science 1999;285:1569-72.

52. Krautwald S, Ziegler E, Tiede K, Pust R and Kunzendorf U. Transduction of the TATFLIP fusion protein results in transient resistance to Fas-induced apoptosis in vivo. J Biol Chem 2004;279:44005-11.

53. Choi JM, Ahn MH, Chae WJ, Jung YG, Park JC, Song HM, et al. Intranasal delivery of the cytoplasmic domain of CTLA-4 using a novel protein transduction domain prevents allergic inflammation. Nat Med 2006;12:574-9.

54. Petronilli V, Miotto G, Marisa B, Raffaele C, Bernardi P and Fabio DL. Transient and long-lasting opening of the mitochondria permeability transient pore can be monitored directly in intact cells by changes in mitochondrial calcein fluorescence. Biophys J 1999;76:725-34.

55. Luca S, Valeria P, Fabio DL, and Paolo B. Commitment to Apoptosis by GD3 Ganglioside Depends on Opening of the Mitochondrial Permeability Transition Pore. J Biol Chem 1999;274:22581-5.

56. Wang GW, Schuschke DA, Kang YJ. Metallothionein overexpressing neonatal mouse cardiomyocytes are resistant to H2O2 toxicity. Am J Physiol 1999;276:167-75.

57. Lee SB, Rao AK, Lee KH, Yang X, Bae YS, Rhee SG. Decreased expression of phospholipase C-beta 2 isozyme in human platelets with impaired function. Blood 1996;88:1684-91.

58. Lipsic E, van der MP, Henning RH, Suurmeijer AJ, Boddeus KM, van Veldhuisen DJ, et al. Timing of erythropoietin treatment for cardioprotection in ischemia/reperfusion. J Cardiovasc Pharmacol 2004;44:473-9.

59. Dhalla NS, Temsah RM, Netticadan T. Role of oxidative stress in cardiovascular diseases. J Hypertens 2000;18:655-73.

60. Tani M. Mechanisms of $Ca^{2+}$ overload in reperfused ischemic myocardium. Annu Rev Physiol 1990;52:543-59.

61. Choi JM, Ahn MH, Chae WJ, Jung YG, Park JC, Song HM, et al. Intranasal delivery of the cytoplasmic domain of CTLA-4 using a novel protein transduction domain prevents allergic inflammation. Nat Med 2006;12:574-9.

62. Kevin LG, Camara AK, Riess ML, Novalija E, Stowe DF. Ischemic preconditioning alters real-time measure of $O_2$ radials in intact hearts with ischemia and reperfusion. Am J Physiol Heart Circ Physiol 2003;284:566-74.

63. Nohl H, Jordan W. The mitochondrial site of superoxide formation. Biochem Biophys Res Commun 1986;138:533-9.

64. Becker LB. New concepts in reactive oxygen species and cardiovascular reperfusion physiology. Cardiovasc Res 2004;61:461-70.

65. Zorov DB, Filburn CR, Klotz LO, Zweier JL, Sollott SJ. Reactive oxygen species (ROS)-induced ROS release: a new phenomenon accompanying induction of the mitochondrial permeability transition in cardiac myocytes. J Exp Med 2000;192:1001-14.

66. Jolly SR, Kane WJ, Bailie MB, Abrams GD, Lucchesi BR. Canine myocardial reperfusion injury. Its reduction by the combined administration of superoxide dismutase and catalase. Circ Res 1984;54:277-85.

67. Masaharu A, Brian O'Rourke, Yasushi T, Jegatheesan S and Eduardo M. Mechanistically Distinct Steps in the Mitochondrial Death Pathway Triggered by Oxidative Stress in Cardiac Myocytes. Circ Res 2003;92:186-194.

68. Chamberlain BK, Volpe P, Fleischer S. Calcium-induced calcium release from purified cardiac sarcoplasmic reticulum vesicles. J Biol Chem 1984;259:7540-6.

69. Osada M, Netticadan T, Tamura K, Dhalla NS. Modification of ischemia-reperfusion-induced changes in cardiac sarcoplasmic reticulum by preconditioning. Am J Physiol Heart Circ Physiol 1998;274:2025-34.

70. Gomez AM, Valdivia HH, Cheng H, Lederer MR, Santana LF, Cannell MB, McCune SA, Altschuld RA, Lederer WJ. Defective excitation-contraction coupling in experimental cardiac hypertrophy and heart failure. Science 1997;276:800-6.

71. Pieske B, Maier LS, Bers DM, Hasenfuss G. $Ca^{2+}$ handling and sarcoplasmic reticulum $Ca^{2+}$ content in isolated failing and nonfailing human myocardium. Circ Res 1999;85:38-46.

72. Allen V, Swigart P, Cheung R, Cockcroft S and Katan M. Regulation of inositol lipid-specific phospholipase-C $\delta$ by changes in $Ca^{2+}$ ion concentrations. Biochem J 1997;327:545-52.

73. Kang SK, Kim DK, Damron DS, Baek KJ and Im MJ. Modulation of intracellular $Ca^{2+}$ via α1B-adrenoreceptor signaling molecules, Gαh (transglutaminase II) and phospholipase C-δ1. Biochem Biophys Res Commun 2002;293:383-90.

74. Yeung HM, Kravtsov GM, Ng KM, Wong TM, Fung ML.Chronic intermittent hypoxia alters $Ca^{2+}$ handling in rat cardiomyocytes by augmented $Na^+/Ca^{2+}$ exchange and ryanodine receptor activities in ischemia-reperfusion. Am J Physiol Cell Physiol. 2007;292:2046-56.

75. Leszek P, Szperl M, Klisiewicz A, Janas J, Biederman A, Rywik T, et al. Alteration of myocardial sarcoplasmic reticulum $Ca^{2+}$-ATPase and $Na^+$-$Ca^{2+}$ exchanger expression in human left ventricular volume overload. Eur J Heart Fail 2007;9:579-86.

76. Mishra S, Sabbah HN, Rastogi S, Imai M, Gupta RC. Reduced sarcoplasmic reticulum $Ca^{2+}$ uptake and increased $Na^+$-$Ca^{2+}$ exchanger expression in left ventricle myocardium of dogs with progression of heart failure. Heart Vessels 2005;20:23-32.

77. Sjaastad I, Bentzen JG, Semb SO, Ilebekk A, Sejersted OM. Reduced

calcium tolerance in rat cardiomyocytes after myocardial infarction. Acta Physiol Scand 2002;175:261-9.

78. Boraso A, Williams AJ. Modification of the gating of the cardiac sarcoplasmic reticulum Ca(2+)-release channel by H2O2 and dithiothreitol. Am J Physiol 1994;267:1010-6.

79. Kawakami M, Okabe E. Superoxide anion radical-triggered $Ca^{2+}$ release from cardiac sarcoplasmic reticulum through ryanodine receptor $Ca^{2+}$ channel. Mol Pharmacol 1998;53:497-503.

80. Anzai K, Ogawa K, Kuniyasu A, Ozawa T, Yamamoto H, Nakayama H. Effects of hydroxyl radical and sulfhydryl reagents on the open probability of the purified cardiac ryanodine receptor channel incorporated into planar lipid bilayers. Biochem Biophys Res Commun 1998;249:938-42.

81. Stephen M and William HF. Protein Kinase C in Cardiac Disease and as a Potential Therapeutic Target. Cardiol Rev 2005;13:3-12.

82. Yigang W and Muhammad A. Role of Protein Kinase C in Mitochondrial KATP Channel–Mediated Protection against $Ca^{2+}$ Overload Injury in Rat

Myocardium. Circ Res 1999;84:1156-65.

83. Tang J, Xie Q, Pan G, Wang J, Wang M. Mesenchymal stem cells participate in angiogenesis and improve heart function in rat model of myocardial ischemia with reperfusion. Eur J Cardiothorac Surg 2006;30:353-61.

84. Sorescu D, Griendling KK. Reactive oxygen species, mitochondria, and NAD(P)H oxidases in the development and progression of heart failure. Congest Heart Fail 2002;8:132-40.

85. Popović ZB, Benejam C, Bian J, Mal N, Drinko J, Lee K, et al. Speckle-tracking echocardiography correctly identifies segmental left ventricular dysfunction induced by scarring in a rat model of myocardial infarction. Am J Physiol Heart Circ Physiol 2007;292:2809-16.

**Abstract (in Korean)**


허혈/재관류 손상에서 Hph1-PLCδ1 단백질의

심근보호효과 및 기전


<지도교수 장 양 수>

연세대학교 대학원 의과학과

임 소 연


허혈/재관류 (ischemia/reperfusion) 손상에 의한 심근 세포의 산화적
손상과 세포내 칼슘의 과부하는 심부전과 같은 심근 기능이상의 발
생 및 진행과 연관되어 있다고 알려져 왔다. Phospholipase C (PLC)는
심장을 포함한 많은 세포에서 phosphoinositol 신호전달기전과 $Ca^{2+}$
항상성의 조절에 중요한 역할을 수행한다. 심근세포에 존재하는

PLC (phospholipase C)의 아형중 한 종류인 δ1은 *in vitro*와 *in vivo*에서 허혈 손상에 의해 증가하는 세포내 칼슘이온의 영향으로 선택적으로 분해됨이 관찰되었다. 본 연구는 허혈시 선택적으로 분해된 PLCδ1 단백질을 재관류 시작시 도입하였을 때 PLCδ1가 어떤 기작을 통하여 허혈/재관류로 인한 손상으로부터 심근보호효과를 나타내는지 관찰하고자 하였다. 이를 위해 세포 투과성 단백질인 Hph1과 PLCδ1의 융합 단백질을 제작하여 허혈/재관류 손상에 대한 치료용 단백질로 사용하였다. Hph1-PLCδ1의 처리는 저산소/재산소화 (hypoxia/ reoxygenation) 손상에 의해 증가된 세포내 칼슘이온의 증가를 감소시켰으며 미토콘드리아의 막 전이소공 (mitochondrial membrane permeability transition pore)의 개방과 막 전위 (mitochondrial membrane potential)의 변화를 억제하였다. 또한 Hph1-PLCδ1는 $H_2O_2$에 의해 자극된 심근세포에서 $Na^+$-$Ca^{2+}$ exchanger and Ryanodine Receptor의 발현에 영향을 미쳤다. 마지막으로 전사멸인자인 Bax, 항사멸인자인 Bcl-2외에 cytochrome C와 caspase 3의 활성을 조절하여 세포사멸을 억제하였다. SD rat 허혈/재관류 모델에서 재관류로부터 2주 경과 후에 심장초음파를 실시했으며 적출한 심장을 이용하여 조직염색을 시행하였다. Hph1-PLCδ1의 주입에 의해 심장의 경색 부위의 크기와 세포 사멸은 유의한 수치로 감소되었고 심장의 수축 및

이완 기능도 개선되었다. 이상의 결과로 Hph1-PLCδ1의 도입이 허혈/재관류 손상시 발생하는 미토콘드리아에 의존적인 세포사멸 경로를 차단함으로써 심근의 기능이상을 완화시킴을 증명하였다.

핵심되는 말: 허혈/재관류, 칼슘 과부하, 산화적 스트레스, Hph1-PLCδ1, 미토콘드리아막 전이 소공, 심근세포

# PUBLICATION LIST

1. Hwang KC, Lim S, Kwon HM, Bae YS, Kang SM, Chung KH, et al. Phospholipase C-$\delta1$ rescues intracellular $Ca^{2+}$ overload in ischemic heart and hypoxic neonatal cardiomyocytes. J Steroid Biochem Mol Biol 2004;91:131-8.